Ringeval, B., Kvakić, M., Augusto, L., Ciais, P., Goll, D. S., Mueller, N. D., Müller, C., Nesme, T., Vuichard, N., Wang, X., Pellerin, S. (2021): Insights on nitrogen and phosphorus co-limitation in global croplands from theoretical and modelling fertilization experiments. - Global Biogeochemical Cycles, 35, 6, e2020GB006915.

DOI: https://doi.org/10.1029/2020GB006915

Title: Insights on nitrogen and phosphorus co-limitation in global croplands from theoretical and modelling fertilization experiments

Bruno Ringeval[1]*, Marko Kvakić[1,2], Laurent Augusto[1], Philippe Ciais[2], Daniel Goll[2], Nathaniel D. Mueller[3,4], Christoph Müller[5], Thomas Nesme[1], Nicolas Vuichard[2], Xuhui Wang[6], Sylvain Pellerin[1]

1 : ISPA, Bordeaux Sciences Agro, INRAE, 33140, Villenave d'Ornon, France.

2 : Laboratoire de Sciences du Climat et de l'Environnement, LSCE/IPSL, CEA-CNRS-UVSQ, Universite Paris-Saclay, Gif-sur-Yvette, France

3 : Department of Ecosystem Science and Sustainability, Colorado State University, Fort Collins, CO, USA

4: Department of Soil and Crop Sciences, Colorado State University, Fort Collins, CO, USA

5 : Potsdam Institute for Climate Impact Research, Member of the Leibniz Association, Potsdam, Germany

6: Sino-French Institute of Earth System Sciences, Peking University, 100871 Beijing, China.

*: corresponding author: bruno.ringeval@inrae.fr, +33 5 57 12 25 05

Running title: Nitrogen and phosphorus co-limitation in global croplands

Key-points:

- Synergistic N and P co-limitation could occur even using the Liebig's law of minimum as the formalism of nutrient interaction.
- By assuming the multiple limitation hypothesis, a true co-limitation could affect ~40% of the global maize area.

Abstract:

Single and combined fertilization additions are a common tool to assess the interactions between nutrients in a given ecosystem. While such experiments can allow systems to be defined into categories of nutrient interactions, e.g. simultaneous co-limitation or single resource response, this categorization may itself be sensitive to way nutrient interactions are mathematically formulated. To this end, we developed a theoretical analysis of nitrogen (N) and phosphorus (P) fertilization experiments based on the computation of ratios between plant demand and soil supply for each nutrient to explore two mathematical interaction formalisms: Liebig's law of minimum (LM) and the multiple limitation hypothesis (MH). We defined, for each interaction formalism, what conditions (in terms of supply and demand in N and P) are required to make the ecosystem in each category of nutrient interaction. Notably, we showed that synergistic co-limitation could occur even using LM formalism under certain conditions. We then applied our framework to global maps of soil nutrient supply and of crop nutrient demand to achieve the potential yield. This was done to examine how the choice of interaction formalism influenced the occurrence of nutrient interaction categories. MH predicts true co-limitation for ~40% of the global maize area where LM predicts other categories of nutrient interaction, particularly single resource P limitation (whose the exact occurrence is, however, sensitive to the amount of P applied in the fertilization experiments). Our study identified areas where real fertilization experiments are required to choose between LM or MH to best represent nutrient interaction in croplands.

Keywords: nutrient limitation, nutrient interaction, Liebig's law, multiple limitation, cropland

1. Introduction

In global assessments of crop ecosystem productivity limitations by nutrients, nitrogen (N) and phosphorus (P) are sometimes considered independently (Peñuelas et al., 2013); or they are considered together but without focusing on how the interaction modulates the limitation (Mueller et al., 2012). N and P cycles interact strongly with different processes that are key to this coupling (Achat et al., 2016). The most commonly studied interaction is related to the limitation of plant growth by nutrients: an increase in organ biomass (mainly composed of carbon, C) requires a given amount of both N and P, to respect stoichiometric constraints. The interaction between C and nutrients is usually represented by C:nutrient ratios for each organ. Plant growth is assumed to be limited when the demand for nutrients, estimated from C:nutrient ratios and C available for potential growth, is not satisfied by the supply of nutrient taken up by the plant. Due to incomplete knowledge about the mechanisms at the basis of the interaction and how these mechanisms are combined when integrating spatial scales and levels of organization (plant organ, individual, community, ecosystem) (Ågren et al., 2012; Davidson A. Eric & Howarth W. Robert, 2007; de Wit, 1992; Sistla & Schimel, 2012), the characterization of multiple element limitation remains an open scientific question. Two formalisms are generally used: Liebig's law of the minimum (LM) or the multiple limitation hypothesis (MH). In LM, plants are assumed to be limited by a single nutrient at a time, with potential release of the nutrient in excess. In MH, it is assumed that plants adjust their growth patterns and thus they are co-limited by multiple nutrients simultaneously (Ågren et al., 2012). The MH formalism thus assumes that plants will mine the least available nutrient by using other resources. For instance, plants growing in an ecosystem with a P-poor soil will invest C and N in the root system (Ryan & Graham, 2018) to access more P

(Davidson A. Eric & Howarth W. Robert, 2007). These investments can take place trough increase in root growth and activity, increase in phosphatase production or fungal mycorrhizae that form symbioses with plant roots and increase in recycling of P within plants (Ryan & Graham, 2018). Both formalisms (LM or MH) could be considered as macro-properties that reflect the same plant adjustments processes but, depending on the conditions, those adjustments may lead to an emerging behaviour that verifies one or the other formalism (Ågren et al., 2012). The further the supply of an essential nutrient deviates from a conceptual and theoretical optimum stoichiometry of plants, the more plants will follow the LM formalism (Ågren et al., 2012). LM is commonly assumed in many studies and is for instance used in most large-scale models dealing with multiple nutrient limitations (Barros et al., 2004; **Folberth et al., 2019**; Goll et al., 2012; Mueller et al., 2012). Despite the representation of some flexibility in allocation and stoichiometry (leading to some flexibility in nutrient requirements), land surface models still apply LM or MH to regulate growth of new tissues (Davies-Barnard et al., 2020).

One way to assess the current nutrient limitation empirically is to provide one-time applications of +N, +P and +NP and to measure the increase in ecosystem productivity as compared to a control trial without any application. Such experiments are usually called fertilization experiments. By definition (Harpole et al., 2011), there is a *true* NP co-limitation when the ecosystem is observed to respond to combined N and P addition only, or to both N and P when added separately. Such co-limitations are (in most cases) synergistic, i.e. the response to +NP is strictly greater than the sum of the responses to +N alone and +P alone. A co-limitation cannot be qualified of *true* (and in that case, is only synergistic) when the ecosystem is insensitive to the addition of one nutrient alone while sensitive to the other one. The different categories of nutrient limitation are summarized in Harpole et al. (2011) and in Table 1. While these categories are commonly used in literature, what each category implies in terms of formalism of nutrient interaction remains unclear. In particular, we aim here to understand which categories are prevented and which ones are more or less promoted by the interaction formalism assumed. To this end, we provided a theoretical framework of N and P fertilization experiments based on the computation of ratios between plant demand and soil supply for each of the two nutrients. The theoretical analysis is developed for two mathematical formalisms of interaction (LM or MH). This allowed us to define, for each formalism, the correspondence between Harpole categories and the values of the limitation by each nutrient when considered alone. Then, we analytically investigated how the choice of formalism modifies the NP limitation.

Finally, we applied our framework to the case of nutrient limitations in croplands. The justification of this choice is twofold: first, nutrient limitation is a key question in croplands at the global scale. Croplands can be over-fertilized but this concerns only few countries in the World. For example, global P fertilizer application in 2005 averaged around 10 kgP/ha/yr but with a large continental variability: ~25kg/ha/yr in Europe vs ~3kg P/ha in Africa (Y. Liu et al., 2008). MacDonald et al. (2011) showed that 30% of cropland are characterized by negative soil P budget. Additional studies have established that nutrient-limitation is a major limitation for croplands at regional (Guilpart et al., 2017; Schils et al., 2018) or at the global scale, besides water limitation. For instance, Mueller et al. (2012) estimated that ~70% of the cropland where potential yield is not achieved at the global scale could close their yield gap by solely focusing on nutrient inputs. The second major reason for focusing on croplands is that experiments with single and combined N and P fertilizer applications (as defining “fertilization experiments”) are not common enough in croplands to provide a global picture of N and P limitation based solely on observations, contrary to what was done in natural ecosystems (Elser et al., 2007; Harpole et al., 2011). Indeed, in cropland, fertilization experiments are usually characterized by an one-time addition for N (Di Paolo & Rinaldi, 2008; Salvagiotti et al., 2008) while for P, the same amount of fertilizer is applied each year for decades in so-called long-term field experiments with crops responding both to the annual supply of fertilizer and to the cumulative effect on soil P availability (e.g. Bai et al. (2013)). This makes deciphering the contribution of each nutrient difficult. Moreover, in such experiments, many P treatments are tested and for a given treatment, the same amount of fertilizer is applied each year for decades, which makes the limitation in the long-term trial somehow non-representative to the nutrient limitation happening in the surrounding fields. When an one-time application is the focus of a study, it is usually difficult to retrieve the application level before the experiment (e.g. Deguchi et al. (2017; Restelatto et al. (2017)), which prevents an accurate definition of the control in these cases. Thus, here, we develop a theoretical analysis, that is particularly suited to investigating nutrient limitations in cropland. We applied our framework on global spatially explicit computations of soil supply and plant demand of N and P for croplands to achieve their potential yield, in order to assess the occurrence of co-limitation in croplands for each interaction formalism. Potential yield is here defined as the theoretical yield achieved without limitations of water and nutrients and without pest/diseases. Thus, water limitation is not considered in the following study and we come back on this point in the discussion.

2. Theoretical framework

Based on a framework commonly used in global studies (Goll et al., 2012; Kvakić et al., 2018), we characterized the limitation of a nutrient considered alone as the ratio (R) of its soil supply (S) and the demand by the plant to achieve its potential biomass (D):

$$R_N = min(1, \frac{S_N}{D_N}) \quad \text{(Eq.1)}$$

$$R_P = min(1, \frac{S_P}{D_P}) \quad \text{(Eq.2)}$$

where S_X and D_X correspond to the supply and demand of the nutrient X, respectively (in kgX/ha/yr) with X is in {N,P}. A ratio R close to 0 means a very high limitation while a ratio close to 1 means no limitation. We prevent R to be greater than 1 as we studied limitation that cannot happen when supply is greater than demand.

Single and combined fertilization experiments are a common tool to assess nutrient limitation on a given site. They correspond to changes in nutrient supply in different combinations from the control (E_1): addition of N alone (E_2), P alone (E_3) or N and P together (E_4) (Fig. 1). Based on the above equations defining the limitations of N and P (Eqs 1 and 2, respectively), theses changes in nutrient supply translate into limitations of each nutrient for each experiment E as follows:

E_1: $R_N(E_1) = min(1, \frac{S_N}{D_N})$ and $R_P(E_1) = min(1, \frac{S_P}{D_P})$ (Eq.3)

E_2: $R_N(E_2) = min(1, \frac{S_N + A_N}{D_N})$ and $R_P(E_2) = min(1, \frac{S_P}{D_P})$ (Eq.4)

E_3: $R_N(E_3) = min(1, \frac{S_N}{D_N})$ and $R_P(E_3) = min(1, \frac{S_P + A_P}{D_P})$ (Eq.5)

E4: $R_N(E_4)=min(1,\frac{S_N+A_N}{D_N})$ and $R_P(E_4)=min(1,\frac{S_P+A_P}{D_P})$ (Eq.6)

with A_N and A_P corresponding to the increase of N and P soil supply following addition of N and P, respectively.

In the above framework, each nutrient is considered alone while the two nutrients interact. An ecosystem is thus defined by its NP limitation, called R_{NP} in the following. Two formalisms of interaction have been here considered to compute R_{NP} from R_N and R_P: multiple limitation hypothesis (called MH in the following, Eq.7) or Liebig's law of the minimum (called LM hereafter, Eq.8):

$$R_{NP\_MH}(E_i)=R_N(E_i).R_P(E_i) \quad \text{(Eq.7)}$$

$$R_{NP\_LM}(E_i)=min(R_N(E_i),R_P(E_i)) \quad \text{(Eq.8)}$$

where E_i is the experiment *i*. In MH, the limitations when the nutrients are considered independently (R_N and R_P) are multiplied to compute the NP limitation while in LM, the smallest one is selected.

We analytically investigated to which extent the choice of the formalism has an effect on the value of R_{NP} for a given (R_N, R_P) couple (Fig. 2a-c). We also investigated how the formalism modulates the increases in R_N and R_P required to alleviate the NP limitation (here represented by an increase in R_{NP} to reach an arbitrary value of 0.75) (Fig. 2d-i). Such increases are called ΔR_N and ΔR_P in the following. ΔR_N and ΔR_P corresponds to the smallest increase in R_N and R_P required at the same time to make R_{NP} equal to 0.75 (Fig. 3). We found that the largest differences in R_{NP} between the LM and MH mathematical formulations are obtained for comparable R_N and R_P values (R_N~R_P) and both within [0.25-0.75] (Fig. 2c). In fact, x in [0.25-0.75] and x~y mathematically maximize the difference between x.y and min(x,y). In addition, the largest differences in ΔR_N between LM and MH occur for $R_N<R_P$ and both R_N and R_P lower than 0.75 (Fig. 2f). Symmetric results are obtained for ΔR_P (Fig. 2i).

In fertilization experiments, nutrient limitation is assessed by looking at the change in productivity (Δpro) according to the addition of P alone (Δpro_{+P}), N alone (Δpro_{+N}) or N and P together (Δpro_{+NP}). Δpro is here not expressed in absolute change but relatively to the potential productivity (i.e. without any limitation). Harpole et al. (2011) defined different categories of limitation when considering the two nutrients in interaction. Each category is entirely defined by: i) the character null or non-null of Δpro_{+N} and Δpro_{+P} and ii) the relationship between Δpro_{+NP} and ($\Delta pro_{+N}+\Delta pro_{+P}$) (i.e. either $\Delta pro_{+NP}>\Delta pro_{+N}+\Delta pro_{+P}$ or $\Delta pro_{+NP}=\Delta pro_{+N}+\Delta pro_{+P}$). N and P are the only ones limiting factors considered: we assumed that other nutrients (as water) are not limiting. Following Harpole et al. (2011), a co-limitation is a synergistic relationship, i.e. there is co-limitation when the increase in productivity following the addition of N and P together is strictly greater than the sum of increases in productivity when each nutrient is added alone (i.e. $\Delta pro_{+NP}>\Delta pro_{+N}+\Delta pro_{+P}$). A given co-limitation is in addition considered as *true* if the responses to +N and +P are either both equal to 0 (i.e. $\Delta pro_{+N}=0$ and $\Delta pro_{+P}=0$, simultaneous co-limitation, category A in Table 1) or both non-null (i.e. $\Delta pro_{+N}\neq 0$ and $\Delta pro_{+P}\neq 0$, independent co-limitation, category B). In other cases (i.e. the ecosystem responses differently to the addition of N and P alone, e.g. $\Delta pro_{+N}=0$ and $\Delta pro_{+P}\neq 0$), the co-limitation cannot be considered as *true* and is only qualified of synergistic (categories C and D in Table 1). Non-synergistic relationship (i.e. $\Delta pro_{+NP}=\Delta pro_{+N}+\Delta pro_{+P}$) concerns the absence of co-limitation: single-resource response (either N or P) or no limitation at all (categories E, F and G in Table 1).

Here, we assumed that the change in productivity following the addition of +N, +P or +NP is equal to the change in R_{NP} following the nutrient addition, i.e.:

$$\Delta\, pro_{+N} = R_{NP}(E_2) - R_{NP}(E_1) \qquad \text{(Eq.9)}$$

$$\Delta\, pro_{+P} = R_{NP}(E_3) - R_{NP}(E_1) \qquad \text{(Eq.10)}$$

$$\Delta\, pro_{+NP} = R_{NP}(E_4) - R_{NP}(E_1) \qquad \text{(Eq.11)}$$

where E_i is the experiment *i* (Fig. 1). This is a key assumption in our approach based on two simplifications described in details in the following. First, through these equations, we assumed that the productivity of a given experiment is proportional to R_{NP} and that the slope of this relationship is equal to 1. In fact, a slope equal to 1 is not necessary to develop the theoretical analysis described in Text S1. As mentioned before, Harpole categories are defined through i) the character null or non-null of Δpro_{+N} and Δpro_{+P} and ii) the relationship between Δpro_{+NP} and (Δpro_{+N}+Δpro_{+P}). These definitions are true even if the productivity of each experiment (and thus the different Δpro) is divided by the same slope. We keep here a slope equal to 1 for the sake of simplicity. Second, Eq.9-11 also imply that the relationship of proportionality between the productivity and R_{NP} is true for all values of R_{NP}, in the range [0-1]. In reality, the productivity vs. limitation relationship is very likely asymptotic (e.g. Bai et al. (2013)). Here, we may approach this non-linearity by assuming a linear relationship for R_{NP} in [0,*thresh*] where *thresh* is a given threshold (lower than 1); followed by a plateau for R_{NP} in [*thresh*,1]. Note that a plateau corresponds to a slope of 0 for the productivity vs. limitation relationship. The correspondence between Harpole categories and the values of R_N and R_P found at the end of our theoretical analysis are still valid in this more general case, but on the restricted range of R_N and R_P values between 0 and *thresh.* In that case, the value 1 used as boundary for R_N and R_P in category definitions – columns 5 and 7 of Table 1 – should be replaced by *thresh*. For the sake of simplicity, we keep in the following *thresh* equal to 1 and come back on this point in the Discussion.

As shown in the column 3 of Table 1, each category of Harpole et al. (2011) could be defined as a combination of: ($\Delta pro_{+N} \neq 0$ or $\Delta pro_{+N} = 0$) AND ($\Delta pro_{+P} \neq 0$ or $\Delta pro_{+P} = 0$) AND ($\Delta pro_{+NP} > \Delta pro_{+N} + \Delta pro_{+P}$ or $\Delta pro_{+NP} = \Delta pro_{+N} + \Delta pro_{+P}$). We manipulated the equations 1 to 11 to translate these properties within implications for nutrient limitations in the control, i.e. $R_N(E_1)$ and $R_P(E_1)$. This allowed us to translate, for each interaction formalism (Eq.7 or 8), the Harpole category definition into conditions on $R_N(E_1)$ and $R_P(E_1)$. This means that we are able to define most Harpole categories in terms of limitation of each nutrient considered alone in the control experiment. $R_N(E_1)$ and $R_P(E_1)$ are respectively called R_N and R_P in the following. The equation manipulation is described in details in Text S1 for both MH and LM. Conclusions of this analysis are summarized in Table 1 (columns 5 for MH and column 7 for LM).

We showed in particular that to belong to the category “independent co-limitation” (category B in Table 1) with MH formalism, an ecosystem has to be characterized by both R_N and R_P in (0,1) (a parenthesis instead of a square bracket used in an interval means here that the corresponding endpoint is excluded from the interval; e.g. R in [0,1) means $0 \leq R < 1$). All other categories (A, C-G) require at least one ratio equal to 0 or 1: e.g. serial limitation N (category C) requires R_N equal to 0 and R_P in (0,1). Categories E,F,G are defined by $\Delta pro_{+NP} = \Delta pro_{+N} + \Delta pro_{+P}$ and we showed that this requires at least one ratio equal to 1 with MH formalism.

We showed that the formalism LM cannot represent true co-limitation, except in the very specific category A (i.e. $R_P=R_N\neq1$). We found that synergistic co-limitation alone (categories C and D) can occur with LM but to be in these categories, the amount of N (if the control is N limited) or P (if the control is P limited) added in the fertilization experiments should be large enough to remove the initial limitation.

3. Sensitivity of co-limitation occurrence to the formalism of interaction in croplands at the global scale

3.1. Methods of computation of spatially explicit R_N and R_P

We computed spatially explicit maps of R_N and R_P in croplands (0.5° latitude x 0.5° longitude) based on the computation of nutrient demand and soil supply. We then applied the previously described theoretical framework on these R_N and R_P values to classify each grid-cell according to Harpole categories for the two interaction formalisms.

The computation of supply and demand maps used to estimate R_N and R_P are described below and in Table 2. To summarize, plant nutrient demand is based on literature-based nutrient harvest index (i.e. the ratio between the nutrient content of grain and the nutrient content of shoot, considered constant at the global scale) combined with spatially explicit distribution of crop potential yield (Y_{pot}) provided by Mueller et al. (2012). The soil N supply has been estimated by using a soil N budget taking into account fertilizer (mineral and organic), atmospheric deposition, biological fixation, and losses by ammoniac volatilization (Bouwman et al., 2013). The soil P supply is assessed by a potential root uptake model that accounts for soil P diffusion and soil P legacy effects. A steady-state assumption was used for N in the stabilized organic matter. Differences in the computation of supply between N and P can be explained by intrinsic differences of behaviour in soils between N ions (NO_3^- and NH_4^+) and orthosphates ions, which are the major forms of N and P taken up by plants (Barber et al., 1963). P is a non-mobile element in soil: ortophosphate ions are easily adsorbed on soil particles which makes its concentration in soil solution very low. In such case, diffusion is the key process of transport in soil. N is much more mobile; its concentration is usually much higher than P concentration and mass flow is the major process of N transport in soil. Given these differences, to representing P supply requires considering the P applied in previous years as well as the soil buffering capacity (i.e. the ability of soil to replenish the soil solution). in contrast, N remaining at the end of the growing season is more likely to be lost through leaching, which prevents us from considering the soil budget of previous years. Supply and demand estimates are representative to a growing season timescale

Following Kvakić et al. (2018), demands for N and P to reach potential yields (D_N and $D_{P,}$ in kg(N or P)/ha/yr) were derived from the combination of i) non-spatially explicit parameters related to the distribution of carbon (C) and nutrients between the different plant organs at maturity found in the literature and ii) spatially explicit potential yield (Y_{pot}, in kgC/ha/yr):

$$D_X = Y_{pot} . \left(\frac{X_{\%,grain}}{XHI} + \frac{X_{\%,root} . RSR}{HI} \right) \quad \text{(Eq.12)}$$

with X in {N,P}. XHI corresponds to the nutrient harvest index (no unit), HI is the harvest index (i.e. the ratio between the carbon content of grain and the carbon content of shoot, no unit), RSR is the root/shoot ratio (no unit) and $X_{\%,grain}$ and $X_{\%,root}$ are nutrient concentrations (kg(N or P)/kgC) for grain and root, respectively. Kvakić et al. (2018) have shown that a XHI-based method provides similar demand estimates compared with other approaches that are based on the nutrient concentration of all plant organs or QUEFTS (Sattari et al., 2014). The definition of the parameters used in Eq.12 (XHI, HI, RSR, $X_{\%,grain}$, $X_{\%,root}$) is based on nutrient and C biomass of different plant organs. Spatially constant values are here used for these parameters. In particular, as the aim of our study is to assess nutrient limitation, we used organ concentrations derived from field experiments in stressed conditions in a multitude of climatic and socio-economic environments (van Duivenbooden, (1992) and Table S1). Details about the computation of Eq.12 and the value of parameters involved in this equation are given in Text S2. The potential yield (Y_{pot}) is provided by Mueller et al. (2012) in tons per hectare. In Mueller et al. (2012), the world grid-cells are divided into climate bins, defined by different combinations of growing degree days and amount of yearly precipitation; and within a climate bin, the potential yield characterizing this bin is defined as the area-weighted 95th percentile of the grid-cell observed yields.

The supply of P (S_P, in kgP/ha/yr) corresponds to the sum of a potential root uptake from P remaining in soils and a prescribed fraction (called α) of the inorganic content of total P fertilizer applied in the year considered (Kvakić et al., 2018).:

$$S_P = \sum_{j=1,12} (A_{root}(j) . P_{uptake}(j)) + \alpha . P_{fert} / CI \qquad \text{(Eq.13)}$$

where j is the month, A_{root} is the monthly root area per unit soil surface area (m^2/ha), $P_{utptake}$ is the monthly potential P root uptake per unit root surface area (kgP/m^2/month), α is constant (unitless), P_{fert} is the inorganic content of total P fertilizer applied the year considered (kgP/ha/yr), and CI is crop harvest per year (unitless). The monthly potential root uptake per unit root surface area (P_{uptake}) is determined by the soil P availability and its diffusion to the root according to the monthly root length density following (Kvakić et al., 2018; Mollier et al., 2008; WILLIGEN & NOORDWIJK, 1994):

$$P_{uptake}(j) = \pi . \Delta z . L_{rv}(j) . D . \frac{\rho^2 - 1}{G(\rho(j), \nu(j))} . C_p \qquad \text{(Eq.14)}$$

where Δz is the soil depth considered (m), L_{rv} is the monthly root length density (m/m^3), D is the coefficient of P diffusion (m^2/month), C_P is the mean concentration of orthophosphate ions of the soil solution in Δz (kgP/m^3), $G(\rho,\nu)$ is a dimensionless geometric function of a ratio of soil cylinder to root radius (ρ, dimensionless) and an uptake of water (ν, dimensionless). In the case of P, for which diffusion is the main process of transport in soil, $G(\rho,\nu)$ is simplified and depends on ρ only. We consider $\Delta z=0.3m$ as P availability and root uptake declines substantially below the plough layer (Lynch & Brown, 2001). The soil solution P concentration C_p was held constant in time and was derived from yearly inorganic labile P provided by Ringeval et al. (2017) following an empirical Freundlich-type relationship described in Kvakić et al. (2018). The global distribution of inorganic labile P was determined by (Ringeval et al., 2017), in which a dynamic soil P model (representing in particular the equilibrium between P bound on soil particles and labile P) was coupled to datasets representing the change in time of soil input/output related to farming practices, atmospheric deposition, land-use change, erosion, etc. The temporal variation of the size of the inorganic labile P pool was represented. The inorganic labile P can accumulate a given year according to both the balance "soil input – soil output" and the soil P dynamic, and can be used by plants in the following years. Thus, we explicitly considered the soil P legacy effect, as it has been shown to be an important process (Ringeval et al., 2014; Sattari et al., 2012). Root characteristics parameters, root biomass at harvest (derived from Y_{pot}, RSR and HI) and seasonality in root biomass (varying between 0 and 1 and derived from simulations of one global gridded crop model, LPJmL (von Bloh et al., 2018)) were combined to compute L_{rv} and A_{root}. As in Kvakić et al. (2018), we assumed that a fraction (α) of the applied fertilizer P is directly available to the plant in the same growing season, thus bypassing the P diffusion pathway. A value of 0.17 is used for α (with an uncertainty of 20%) based on (Balemi & Negisho, 2012). Further details can be found in the supporting information (Text S3).

For the supply of N, we used a simpler approach justified by the higher mobility of N in soil than P. We assumed that the transport of N in soil to the root is not limiting in the case of N as its larger concentration makes mass flow efficient. Equation 14 could be applied to the uptake of any solute in the soil, but in the case of a solute whose the transport happens through mass flow, the geometry function G depends not only to root geometry (ρ) but also to water uptake (v). This would require the representation of water transpiration by plant, which was considered out of the scope of our study. Higher mobility of N allows us to neglect legacy effects. With the exception of few recent studies (e.g. ten Berge et al., 2019, focusing on sub-Saharan Africa), N applied in previous years is commonly neglected in global modelling approaches (A. F. Bouwman et al., 2017; Conant et al., 2013; Lassaletta et al., 2014; J. Liu et al., 2010). The supply of N is calculated from the soil N input of the year considered (chemical and organic fertilizer, atmospheric deposition, symbiotic fixation, crop residues remaining on/within crop soils) minus losses corresponding to NH_3 volatilization and leaching:

$$S_N = N_{fix} + N_{dep} + N_{fert} + N_{man} + N_{res} - N_{vol} - N_{leach} \quad \text{(Eq.15)}$$

where N_{fix}, N_{dep}, N_{fert}, N_{man}, N_{res} are soil N inputs corresponding to symbiotic fixation, deposition, chemical fertilizer, manure applied on cropland soil, and crop residues respectively. N_{vol} and N_{leach} are soil outputs corresponding to NH_3 volatilization and leaching. Datasets describing N_{fix}, N_{dep}, N_{fert}, N_{man}, and N_{vol} were provided by Bouwman et al. (2013). N_{res} includes root biomass if the harvest is aboveground and was computed from N in harvest given by Bouwman et al. (2013) and global parameters (ratios between plant uptake and harvest and between residues remaining on the field and total residues) based on Smil, 1999 (see Text S4). A similar computation was done to estimate N in crop residues in Liu et al. (2010) and for P in crop residues in Ringeval et al. (2017).

In reality, not all crop residues and manure applied on soil enhances the soil mineral N at the year of application; only a labile fraction (which depends on the manure type and C:N ratio of the residues) can be used by plants the year of application (Chadwick et al., 2000; Trinsoutrot et al., 2000) while a stable fraction enriches a pool of stabilized N organic matter. The stabilized organic N is mineralized in the following years, contributing to enhance the mineral N. Soil organic N consists also in a microbial pool which is connected to the stabilized organic N and with the mineral N (immobilization/mineralization). Here, the microbial pool was neglected and we assumed that the stabilized organic matter is in steady-state. This allows us to consider that all crop residues and manure applied on/within the soils a given year reach S_N without distinguishing the labile vs. stable fractions of residues and manure. An assumption of steady-state was also used in (L. Bouwman et al., 2013) and in (J. Liu et al., 2010).

N leaching was computed following the IPCC (Hergoualc'h, 2019): N_{leach} was assumed to be equal to 24% of input of fertilizer (chemical + manure) for grid-cells where the annual precipitation is greater than annual potential evapotranspiration and null elsewhere. IPCC-computed leaching is likely overestimated but an alternative computation (Wang et al., 2019) had a limited effect on our results (not shown). Annual precipitation and potential evapotranspiration were provided by CRU (Harris et al., 2020).

We recognize that the use of constant parameters at the global scale in the computation of supply and demand is a substantial simplification (Hay, 1995; Sadras, 2006). This is particularly true with respect to plant adjustments to nutrient limitations (Colomb et al., 2007) which are susceptible to modify nutrient organ concentrations. Cultivar diversity also leads to real world differences, e.g., for HI. However, both plant adjustments (O. Franklin et al., 2012) and the effect of cultivar diversity on allocation (Folberth et al., 2016) are difficult to represent at the global scale. It is also worth noting that, despite using constant parameters at the global scale, considering grid-cells independently in our uncertainty analysis (see below) made these parameters artificially vary in space.

Each term (S_N, D_N, S_P, D_P) is spatially explicit at half-degree resolution. We took an uncertainty associated with the supply and demand variables into account. To do this, we computed 1000 replicates for each variable (S_N, D_N, S_P, D_P) by considering different sources of uncertainty (Table 2). Grid-cells are considered independently within each replicate. These replicates were then used pairwise to compute 1000 replicates for R_N, R_P and R_{NP}. For each ratio, an average and a standard-deviation among these replicates were computed for each grid-cell and were plotted as 2D maps in Supporting Figures. In addition, two values are given to provide information at the global scale: the average and the standard-deviation of the 1000 global averages. Each global average is computed by using the grid-cell crop area (Ramankutty et al., 2008) as weight. Maize, rice and wheat are considered in this study (see the crop-dependent terms in Table 2) and the ratios computed are representative of the year 2000. Only grid-cells for which R_P and R_N could be computed are considered, which determines the crop area and the global crop production considered in our study (Table S2). In the Main Text, a specific focus is made on maize because it is the most widespread crop across latitudes.

3.2. Effects of formalism choice on global NP limitation

Spatial distributions of R_N, R_P as well as R_{NP} computed with both formalisms are described and discussed in Text S5. The relationship between R_{NP} and actual yield gap provided by statistical approaches (Y_{real}/Y_{pot}, with Y_{real} being the actual yield) has been investigated at country scale (Text S6). The uncertainty at the grid-cell scale, arising from the uncertainty in the datasets and equation parameters, is larger for P than for N (Fig. S4), which reflects the large uncertainty in the P supply (Table S3). Nevertheless, the uncertainty regarding global values remains small (Table 3). Given the large uncertainty at grid-cell scale, we did not focus our analysis on the exact distribution of R_N and R_P. Instead, we assess how the choice of formalism has an effect on R_{NP}, ΔR and the occurrence of Harpole categories at the global scale. Obviously, the effect of formalism choice on the global values of R_{NP}, ΔR_N and ΔR_P depends on the distribution of grid-cells in the (R_N, R_P) space (grey dots in Fig. 2c,f,i). Even though significant, the difference between LM and MH in global R_{NP} is small (Table 3). This is explained by a small number of grid-cells (~3%) characterized by conditions that maximize the difference between the LM and MH mathematical formulations (i.e. comparable $R_N \sim R_P$ and both within [0.25-0.75], see above). Finally, ~60% of the grid-cells are characterized by a difference LM – MH smaller than the uncertainty computed with a given formalism (LM or MH).

The global averages of ΔR computed with MH ($\Delta R_N=0.36\pm0.00$, $\Delta R_P=0.30\pm0.01$) are larger than those computed with LM ($\Delta R_N=0.30\pm0.00$, $\Delta R_P=0.26\pm0.01$). Numbers provided correspond to averages and standard-deviations among 1000 replicates of global averaged R_N and R_P. It was analytically shown (Fig. 2) that the LM – MH difference of ΔR_P is maximal for a combination of small R_P and medium R_N, as encountered in the centre of the USA (Text S5 and Fig. S4). Large differences are also noticeable in regions with high limitations of both nutrients, such as the Western Russian Federation and Ukraine.

3.3. Effects of formalism choice on occurrence of Harpole categories

We computed the occurrence of each Harpole category by using conditions in terms of R_N and R_P, as described in Table 1. We checked that these occurrences are equal to the occurrences found when: modelling fertilization experiments are performed, R_{NP} are computed for each experiment (Eq.7-8) and Eq.9-11 are then applied. The increase of N and P supply (A_N and A_P) in fertilization experiments are here equal to 30kgN/ha/yr and 5kgP/ha/yr, respectively and are spatially homogeneous for all cropland around the World. While our theoretical framework was initially developed for productivity (Section 3.2), we applied it here to cropland yield, which is consistent with the assumption of fixed harvest index as described in Section 3.1.

With the formalism MH, we found that true co-limitation occurs in 38.2±0.6 % of the global crop area for maize, via independent co-limitation (category B in Table 1). This category is found in the USA, South America, the Western Russian Federation and Ukraine (Fig. 4a). As showed theoretically, to belong to that category a crop has to be characterized by both R_N and R_P in (0,1). In our simulations, these conditions occur for ~38% of the maize crop area. Synergistic co-limitation alone (categories C and D) occurs for 6.8±0.3 % of the global maize crop area and this is only explained by serial limitation N (category C, dark blue in Fig. 4a): no serial limitation P was found in our numerical application. This can be explained by the fact that R_P (contrary to R_N) is never null in our simulations because of the soil P legacy taken into account in our approach (Ringeval et al., 2017). This also prevents simultaneous co-limitation (A) from being found. The occurrence of true co-limitation at the global scale varies between crops (38.2±0.6 % for maize, 30.6±0.4 % for wheat and 14.8±0.8 % for rice, not shown). Except for few regions (e.g. India), grid-cells where the three crops are grown belong to the same limitation category for all crops (not shown): the difference in occurrence of co-limitation between crops is mainly explained by the crop-specific global distribution.

As theory shows (Text S1), the formalism LM cannot represent true co-limitation, except in the very specific category A (i.e. $R_P=R_N\neq1$), which is never encountered in our study (Fig. 4b and Table 1). We found that synergistic co-limitation alone (categories C and D) can occur in more than 12% of the global maize area with LM. However, this number is sensitive to the amount of N and P added in the fertilization experiments (called respectively A_N and A_P in Fig. 1). E.g. a cropland which is initially P-limited is classified in the category D if the amount of P added (A_P) is sufficient to remove the P limitation (i.e. the cropland becomes N limited); otherwise, it belongs to the category F (Table 1).

Figure 4 shows that many areas are characterized by the same category whatever the interaction formalism chosen (LM or MH): e.g. single-resource limitation N (category E) in Europe, no response to either N or P or NP additions (category G) in India and west of China. The most noticeable differences between LM and MH appear in areas where MH predicts independent co-limitation (category B) while LM predicts other categories. In particular, 62% of the global maize area considered as B with MH belongs to single-resource response P (category F) while 19% belongs to serial limitation P (category D) but the partition of F vs. D depends on the amount of P added in the fertilizer experiment (called A_P in Eq.5-6). These areas of mismatch between MH and LM encompass USA, South America, the Western Russian Federation and Ukraine (Fig.4). Following these results, real fertilization experiments in these areas would help to choose between LM or MH to best represent nutrient interaction.

4. Discussion

Our work clarifies the mathematical conditions in terms of supply/demand ratios required to place an ecosystem into a category of nutrient limitation, as defined by Harpole et al. (2011). In particular, we found that synergistic co-limitation can occur with Liebig's law of the minimum under certain conditions that are functions of the amount of N and P added in fertilization experiments, as already suggested by Ågren et al. (2012). While Liebig's law of the minimum is based on the limitation by a single nutrient at a time, it allows synergistic co-limitation to happen, which could be counter-intuitive. We found that, if multiple limitation hypothesis is the most appropriate way to represent nutrient interaction, co-limitation should occur for ~46% of the maize crop area (38% of true and synergistic co-limitation + 7% for synergistic alone co-limitation). The occurrence of true co-limitation in croplands would be of a similar magnitude to those reported for natural ecosystems (28% in Harpole et al. (2011), 42% in Augusto et al. (2017)).

More investigations are needed to precise the real occurrence of co-limitation in croplands. To do so, a method based on observations, as performed for natural ecosystems (Harpole et al., 2011), is required. As mentioned in the Introduction, one-time fertilizer applications are not as common in croplands as in natural ecosystems. Or at least, they exist but are exploitable with difficulties. A huge work is required to select studies that deal with one-time applications for both nutrients (alone and in combination), that provide information about the previous applications (that determines the control), and that are characterized by a control that is representative to the region where the trial occurs. A part of the work has been recently done by (Hou et al., 2020) .

Contrary to previous meta-analysis of fertilization experiments that focused on natural ecosystems only (Augusto et al., 2017; Elser et al., 2007; Li et al., 2016; Yue et al., 2017), the study of Hou et al. (2020) included cropland. However, it treats exclusively of P and neither of N nor of interaction between N and P. In addition, more work is needed to select studies that can be used based on a well-defined and region-representative control. Once these studies have been selected, they can be compiled. If numerous enough, they would tell us if co-limitation is really common in croplands, suggesting e.g. that farming practices tend to promote co-limitation. On the opposite, the absence of such co-limitation would suggest that human perturbation of nutrient cycles pushes the crop plant outside of its adaptation capacity. Contrary to what happens in natural ecosystems, change in the plant community cannot occur consecutively to fertilizer application in cropland systems as they are mostly single crop. Thus, co-limitation in cropland should be considered as reflecting plant adaptations, e.g.: plant can invest nutrient in excess to access the limiting nutrient. And an absence of co-limitation would suggest that plant cannot adapt to perturbations. A map of co-limitation based on real fertilization experiments would be different to the spatial distributions of occurrence found in our study (Fig.4) as each interaction formalism used here remains a rough plant-scale approximation of the balance between few plant adjustments.

The occurrences of the different limitation categories that we provided are a function of the spatial distribution of R_N and R_P, as posited by our theoretical framework. However, these maps are prone to uncertainty due to simplifications in our modelling approach. As mentioned in Section 3.1, some simplifications are related to the use of constant parameters at the global scale in the computation of supply and demand while plant adjustments and some farming practices are susceptible to modify them. Global changes are also very likely modifying yield and grain composition (e.g. Long et al., 2006; Müller et al., 2014) and this effect was not considered in our study which does not simulate temporal changes in nutrient limitation. Our computation of supply in N and P are also prone to large uncertainties. For instance, the root P uptake model is quite simple. The soil solution P concentration does not seasonally vary and its relationship with inorganic labile P describes the long-term equilibrium while seasonal dynamic should be considered, in particular for high fixing capacity soils (e.g. oxisols) or soils that precipitate phosphate (e.g. soils with carbonate). This limitation is evident in our treatment of fertilizer P (see Eq.13 and (Kvakić et al., 2018)). Some key processes that increase P acquisition (Hinsinger et al., 2011) like root branching/architecture, exudates/ phosphatase, and mycorrhizae association are also neglected. Our soil supply of N is very simple and an explicit representation of stabilized N organic matter and inclusion of microbial N would be an interesting addition for future research. Also, we consider that all N available can be used by plants, while it should instead be seen as a pool from which different users (plants, denitrifying bacteria and percolating water) take N. Competition between plants and microbes is only beginning to be implemented in land surface models (Davies-Barnard et al., 2020). Seasonality in N supply could be also considered, as N leaching likely concerns the N remaining at the end of the growing season and not N taken up by plants (De Jong et al., 2009). Another simplification is related to the use of potential yield provided by statistical methods based on maximum attainable yield within climate bins (Mueller et al., 2012). Such approaches have difficulty distinguishing irrigated and rainfed crops and thus, the here used Y_{pot} could be in fact water-limited in some places (van Ittersum et al., 2013). The statistical methodology has been recently updated to improve the separation between water-limited and irrigated yield potential (Wang et al. 2021). Alternative estimates of potential yield such as the ones simulated by

Global Gridded Crop Models are also prone to huge uncertainties (Müller et al., 2017; Bruno Ringeval et al., 2021).

In our approach, the limitation of *potential* yield is computed by considering current farming practices to derive the supply. Current practices could be influenced by other limiting factors: e.g. if a crop is water limited, farmers can adapt their practices and reduce their nutrient applications accordingly. Sensitivity tests where the demand would be derived from actual yield (instead of potential yield, as in the Main Text) show that R_{NP} slightly increases, from ~0.35 (as in Table 2) to ~0.45. More interesting, such sensitivity tests could help in the determination of areas where other limiting factors (including water) might play a role (Fig. S2). The next step is to consider more limiting factors together with the issue to represent their interaction.

Our theoretical analysis has also few caveats. In particular, we assumed a linear relationship between R_{NP} and the productivity of each experiment (Eq. 9-11). As underlined in the method section, our conclusions are still valid if we assumed a linear relationship up to a value *thresh* if *thresh* replaces 1 in the definition categories given in Table 1. The value *thresh* is nevertheless theoretical because the calculated nutrient limitation (R_N, R_P, R_{NP}) has no physical meaning and is disconnected from physical measure of e.g. soil P content (Olsen P, etc.). The fact that the transition between linear and plateau regimes occurs for the same R_{NP} (1 or *thresh*) globally should be an acceptable assumption as we took into account the spatial variation in soil properties to compute the soil nutrient supply.

In our analysis, we computed ΔR_N and ΔR_P, i.e. the increase in R_N and R_P required to increase R_{NP} up to 0.75 and assessed how the choice of the interaction formalism has an effect on ΔR_N and ΔR_P. The variables ΔR_N and ΔR_P could be translated to increase in soil supply by considering nutrient demand in each grid-cell. However such change in supply cannot be easily translated into a change in fertilizer, since our supply estimates take into account some processes occurring after the fertilizer application: for P, we take into account the dynamics of P in soil (diffusion and root uptake) while for N, we allow for NH_3 volatilization and leaching. Our nutrient requirement calculation is driven solely by nutrient limitation, independently of yield gap, contrary to previous estimates based on: soil quality indicators (with no distinction between N and P) (Fischer et al., 2012; Pradhan et al., 2015), statistical relationships between fertilizer application and yield (Mueller et al., 2012) or “N uptake gaps” based on yield gap and minimal/maximal values of the physiological N efficiency in aboveground biomass derived from the QUEFTS model (Schils et al., 2018; ten Berge et al., 2019). More generally, our nutrient limitation is not straight connected to the yield gap because the actual yield is not used in our computation. It is interesting to note that our computation of ΔR_N and ΔR_P is based on the minimum “physiological” needs for plants. Behind the multiple limitation's mathematical formalism, an increase in R_{NP} can be achieved for different combinations of increases in N and P (i.e. for different couples (ΔR_N, ΔR_P)): despite non-substitution at the molecular or cellular level (Sinclair & Park, 1993), one element can partly compensate for the other at the plant scale. Here, we considered only one couple (Fig. 3), while external variables such as the price or the ease of access to fertilizers will also influence the farmer's choice and could make him/her select another NP combination. This should be taken into account in future attempts to make link with scenarios of nutrient management and policy more straightforward.

Two formalisms are usually used to characterize multiple element limitation: in Liebig's law of the minimum, plants are generally limited by one nutrient at a time, while plants are generally co-limited in a multiple limitation hypothesis. Our study reveals that the choice of the formalism has only a marginal effect on the estimate of current global NP limitation (R_{NP}) for the cereals considered. This result is explained by the fraction of grid-cells in our approach that is within the area of the R_N vs R_P space that maximizes the difference between the two formalisms. The formalism choice has a bigger effect on the increases in R_N and R_P required at the same time to alleviate the NP limitation. Because of very different theoretical founding principles behind each formalism, the use of one or other formalism leads to very different estimates of occurrence of co-limitation (i.e. the occurrence of each category defined in Table 1) in cropland. Our study identifies areas where real fertilization experiments should occur to help choosing between LM or MH to best represent nutrient interaction in croplands. Other option is to go further in the representation of mechanisms of nutrient interaction in models. Indeed, as mentioned earlier, Liebig's law of minimum or multiple limitation hypothesis could be considered as macro-properties that reflect the same processes of plant adjustments but, depending on the context, plant adjustments lead to one or the other formalism (Ågren et al., 2012). It was also stipulated (Farrior et al., 2013) that plants can be limited by only one resource at a time, but that the integration of the different limitations in time makes the plants limited by several resources at the scale of the growing season. In our point of view, the use of mechanistic approaches as the ones based on optimality principles (Oskar Franklin et al., 2020) combined with floating C:nutrients ratios (Zaehle & Dalmonech, 2011) would allow the explicit consideration of some plant adjustments, preventing the need to choose between formalisms.

References

Achat, D. L., Augusto, L., Gallet-Budynek, A., & Loustau, D. (2016). Future challenges in coupled C–N–P cycle models for terrestrial ecosystems under global change: a review. *Biogeochemistry*, *131*(1-2), 173–202. https://doi.org/10.1007/s10533-016-0274-9

Ågren, G. I., Wetterstedt, J. Å. M., & Billberger, M. F. K. (2012). Nutrient limitation on terrestrial plant growth - modeling the interaction between nitrogen and phosphorus. *New Phytologist*, *194*(4), 953–960. https://doi.org/10.1111/j.1469-8137.2012.04116.x

Augusto, L., Achat, D. L., Jonard, M., Vidal, D., & Ringeval, B. (2017). Soil parent material-A major driver of plant nutrient limitations in terrestrial ecosystems. *Global Change Biology*. https://doi.org/10.1111/gcb.13691

Bai, Z., Li, H., Yang, X., Zhou, B., Shi, X., Wang, B., et al. (2013). The critical soil P levels for crop yield, soil fertility and environmental safety in different soil types. *Plant and Soil*, *372*(1-2), 27–37. https://doi.org/10.1007/s11104-013-1696-y

Balemi, T., & Negisho, K. (2012). management of soil phosphorus and plant adaptation mechanisms to phosphorus stress for sustainable crop production: a review. Journal of Soil Science and Plant Nutrition, 16.

Barber, S. A., Walker, J. M., & Vasey, E. H. (1963). Mechanisms for Movement of Plant Nutrients from Soil and Fertilizer to Plant Root. Agricultural and Food Chemistry, 11(3), 204–207.

Barros, I. de, Williams, J. R., & Gaiser, T. (2004). Modeling soil nutrient limitations to crop production in semiarid NE of Brazil with a modified EPIC version. *Ecological Modelling*, *178*(3-4), 441–456. https://doi.org/10.1016/j.ecolmodel.2004.04.015

ten Berge, H. F. M., Hijbeek, R., van Loon, M. P., Rurinda, J., Tesfaye, K., Zingore, S., et al. (2019). Maize crop nutrient input requirements for food security in sub-Saharan Africa. *Global Food Security*, *23*, 9–21. https://doi.org/10.1016/j.gfs.2019.02.001

Von Bloh, W., Schaphoff, S., Müller, C., Rolinski, S., Waha, K., & Zaehle, S. (2018). Implementing the nitrogen cycle into the dynamic global vegetation, hydrology, and crop growth model LPJmL (version 5.0). *Geoscientific Model Development*, *11*(7), 2789–2812. https://doi.org/10.5194/gmd-11-2789-2018

Bouwman, L., Goldewijk, K. K., Van Der Hoek, K. W., Beusen, A. H. W., Van Vuuren, D. P., Willems, J., et al. (2013). Exploring global changes in nitrogen and phosphorus cycles in agriculture induced by livestock production over the 1900-2050 period. *Proceedings of the National Academy of Sciences USA*, doi: 10.1073/pnas.1012878108. https://doi.org/10.1073/pnas.1012878108

Bouwman, L., Beusen, A. H. W., Lassaletta, L., van Apeldoorn, D. F., van Grinsven, H. J. M., Zhang, J., & Ittersum van, M. K. (2017). Lessons from temporal and spatial patterns in global use of N and P fertilizer on cropland. *Scientific Reports*, *7*, 40366. https://doi.org/10.1038/srep40366

Chadwick, D. R., John, F., Pain, B. F., Chambers, B. J., & Williams, J. (2000). Plant uptake of nitrogen from the organic nitrogen fraction of animal manures: a laboratory experiment. *The Journal of Agricultural Science*, *134*(2), 159–168. https://doi.org/10.1017/S0021859699007510

Colomb, B., Debaeke, P., Jouany, C., & Nolot, J. M. (2007). Phosphorus management in low input stockless cropping systems: Crop and soil responses to contrasting P regimes in a 36-year experiment in southern France. *European Journal of Agronomy*, *26*(2), 154–165. https://doi.org/10.1016/j.eja.2006.09.004

Conant, R. T., Berdanier, A. B., & Grace, P. R. (2013). Patterns and trends in nitrogen use and nitrogen recovery efficiency in world agriculture. *Global Biogeochemical Cycles*, *27*(2), 558–566. https://doi.org/10.1002/gbc.20053

Davidson, A. E., & Howarth, W. R. (2007). Nutrient in synergy. *Nature*, *449*(7165), 1000.

Davies-Barnard, T., Meyerholt, J., Zaehle, S., Friedlingstein, P., Brovkin, V., Fan, Y., et al. (2020). Nitrogen cycling in CMIP6 land surface models: progress and limitations. *Biogeosciences*, *17*(20), 5129–5148. https://doi.org/10.5194/bg-17-5129-2020

Deguchi, S., Uozumi, S., Touno, E., Uchino, H., Kaneko, M., & Tawaraya, K. (2017). White clover living mulch reduces the need for phosphorus fertilizer application to corn. *European Journal of Agronomy*, *86*, 87–92. https://doi.org/10.1016/j.eja.2017.03.006

van Duivenbooden, N. (1992). *Sustainability in terms of nutrient elements with special reference to West-Africa*. Wageningen: CABO-DLO. Retrieved from http://edepot.wur.nl/332997

Elser, J. J., Bracken, M. E. S., Cleland, E. E., Gruner, D. S., Harpole, W. S., Hillebrand, H., et al. (2007). Global analysis of nitrogen and phosphorus limitation of primary producers in freshwater, marine and terrestrial ecosystems. *Ecology Letters*, *10*(12), 1135–1142. https://doi.org/10.1111/j.1461-0248.2007.01113.x

Farrior, C. E., Tilman, D., Dybzinski, R., Reich, P. B., Levin, S. A., & Pacala, S. W. (2013). Resource limitation in a competitive context determines complex plant responses to experimental resource additions. *Ecology*, *94*(11), 2505–2517.

Fischer, G., Nachtergaele F.O., Prieler S., Teixeira E., Toth G., van Velthuizen H., et al. (2012). Global Agro_ecological Zones (GAEZ ver 3.0), Model documentation. IIASA/FAO.

Folberth, C., Elliott, J., Müller, C., Balkovic, J., Chryssanthacopoulos, J., Izaurralde, R. C., et al. (2016). Uncertainties in global crop model frameworks: effects of cultivar distribution, crop management and soil handling on crop yield estimates. *Biogeosciences Discussions*, 1–30. https://doi.org/10.5194/bg-2016-527

Folberth, C., Elliott, J., Müller, C., Balkovič, J., Chryssanthacopoulos, J., Izaurralde, R. C., Jones, C. D., Khabarov, N., Liu, W., Reddy, A., Schmid, E., Skalský, R., Yang, H., Arneth, A., Ciais, P., Deryng, D., Lawrence, P. J., Olin, S., Pugh, T. A. M., Ruane, A. C., and Wang, X., (2019) Parameterization-induced uncertainties and impacts of crop management harmonization in a global gridded crop model ensemble, edited by: Martínez-Paz, J. M., PLOS ONE, 14, e0221862, https://doi.org/10.1371/journal.pone.0221862

Franklin, O., Johansson, J., Dewar, R. C., Dieckmann, U., McMurtrie, R. E., Brannstrom, A., & Dybzinski, R. (2012). Modeling carbon allocation in trees: a search for principles. *Tree Physiology*, *32*(6), 648–666. https://doi.org/10.1093/treephys/tpr138

Franklin, O., Harrison, S. P., Dewar, R., Farrior, C. E., Brännström, Å., Dieckmann, U., et al. (2020). Organizing principles for vegetation dynamics. Nature Plants, 6(5), 444–453. https://doi.org/10.1038/s41477-020-0655-x

Goll, D. S., Brovkin, V., Parida, B. R., Reick, C. H., Kattge, J., Reich, P. B., et al. (2012). Nutrient limitation reduces land carbon uptake in simulations with a model of combined carbon, nitrogen and phosphorus cycling. *Biogeosciences*, *9*(9), 3547–3569. https://doi.org/10.5194/bg-9-3547-2012

Guilpart, N., Grassini, P., van Wart, J., Yang, H., van Ittersum, M. K., van Bussel, L. G. J., et al. (2017). Rooting for food security in Sub-Saharan Africa. *Environmental Research Letters*, *12*(11), 114036. https://doi.org/10.1088/1748-9326/aa9003

Harpole, W. S., Ngai, J. T., Cleland, E. E., Seabloom, E. W., Borer, E. T., Bracken, M. E. S., et al. (2011). Nutrient co-limitation of primary producer communities: Community co-limitation. *Ecology Letters*, *14*(9), 852–862. https://doi.org/10.1111/j.1461-0248.2011.01651.x

Harris, I., Osborn, T. J., Jones, P., & Lister, D. (2020). Version 4 of the CRU TS monthly high-resolution gridded multivariate climate dataset. Scientific Data, 7(109).

Hay, R. K. M. (1995). Harvest index: a review of its use in plant breeding and crop physiology. *Ann. Appl. Biol*, pp. 197–216.

Hergoualc'h, K. (2019). Chapter 11: N 2 O Emissions from Managed Soils, and CO 2 Emissions from Lime and Urea Application. In *2019 Refinement to the 2006 IPCC Guidelines for*

National Greenhouse Gas Inventories. Retrieved from https://www.ipcc-nggip.iges.or.jp/public/2019rf/pdf/4_Volume4/19R_V4_Ch11_Soils_N2O_CO2.pdf

Hinsinger, P., Brauman, A., Devau, N., Gérard, F., Jourdan, C., Laclau, J.-P., et al. (2011). Acquisition of phosphorus and other poorly mobile nutrients by roots. Where do plant nutrition models fail? *Plant and Soil*, *348*(1–2), 29–61. https://doi.org/10.1007/s11104-011-0903-y

Hou, E., Luo, Y., Kuang, Y., Chen, C., Lu, X., Jiang, L., et al. (2020). Global meta-analysis shows pervasive phosphorus limitation of aboveground plant production in natural terrestrial ecosystems. Nature Communications, 11(1), 637. https://doi.org/10.1038/s41467-020-14492-w

van Ittersum, M. K., Cassman, K. G., Grassini, P., Wolf, J., Tittonell, P., & Hochman, Z. (2013). Yield gap analysis with local to global relevance—A review. *Field Crops Research*, *143*, 4–17. https://doi.org/10.1016/j.fcr.2012.09.009

De Jong, R., Drury, C. F., Yang, J. Y., & Campbell, C. A. (2009). Risk of water contamination by nitrogen in Canada as estimated by the IROWC-N model. Journal of Environmental Management, 90(10), 3169–3181. https://doi.org/10.1016/j.jenvman.2009.05.034

Kvakić, M., Pellerin, S., Ciais, P., Achat, D. L., Augusto, L., Denoroy, P., et al. (2018). Quantifying the Limitation to World Cereal Production Due To Soil Phosphorus Status. *Global Biogeochemical Cycles*. https://doi.org/10.1002/2017GB005754

Lassaletta, L., Billen, G., Grizzetti, B., Anglade, J., & Garnier, J. (2014). 50 year trends in nitrogen use efficiency of world cropping systems: the relationship between yield and nitrogen input to cropland. *Environmental Research Letters*, *9*(10), 105011. https://doi.org/10.1088/1748-9326/9/10/105011

Li, Y., Niu, S., & Yu, G. (2016). Aggravated phosphorus limitation on biomass production under increasing nitrogen loading: a meta-analysis. Global Change Biology, 22(2), 934–943. https://doi.org/10.1111/gcb.13125

Liu, Y., Villalba, G., Ayres, R. U., & Schroder, H. (2008). Global Phosphorus Flows and Environmental Impacts from a Consumption Perspective. *Journal of Industrial Ecology*, *12*(2), 229–247. https://doi.org/10.1111/j.1530-9290.2008.00025.x

Liu, J., You, L., Amini, M., Obersteiner, M., Herrero, M., Zehnder, A. J. B., & Yang, H. (2010). A high-resolution assessment on global nitrogen flows in cropland. Proceedings of the National Academy of Sciences, 107(17), 8035–8040. https://doi.org/10.1073/pnas.0913658107

Long, S. P., Ainsworth, E. A., Leakey, A. D., Nösberger, J., & Ort, D. R. (2006). Food for Thought: Lower-Than-Expected Crop Yield Stimulation with Rising CO. *Science*, *312*.

Lynch, J. P., & Brown, K. M. (2001). Topsoil foraging–an architectural adaptation of plants to low phosphorus availability. *Plant and Soil*, *237*(2), 225–237.

MacDonald, G. K., Bennett, E. M., Potter, P. A., & Ramankutty, N. (2011). Agronomic phosphorus imbalances across the world's croplands. *Proceedings of the National Academy of Sciences USA*, *108*(7), 3086–3091. https://doi.org/10.1073/pnas.1010808108

Mollier, A., De Willigen, P., Heinen, M., Morel, C., Schneider, A., & Pellerin, S. (2008). A two-dimensional simulation model of phosphorus uptake including crop growth and P-response. Ecological Modelling, 210(4), 453–464. https://doi.org/10.1016/j.ecolmodel.2007.08.008

Mueller, N. D., Gerber, J. S., Johnston, M., Ray, D. K., Ramankutty, N., & Foley, J. A. (2012). Closing yield gaps through nutrient and water management. *Nature*, *490*(7419), 254–257. https://doi.org/10.1038/nature11420

Müller, C., Elliott, J., & Levermann, A. (2014). Food security: Fertilizing hidden hunger. *Nature Climate Change*, *4*(7), 540.

Müller, C., Elliott, J., Chryssanthacopoulos, J., Arneth, A., Balkovic, J., Ciais, P., et al. (2017).

Global gridded crop model evaluation: benchmarking, skills, deficiencies and implications. *Geoscientific Model Development*, *10*(4), 1403–1422. https://doi.org/10.5194/gmd-10-1403-2017

Di Paolo, E., & Rinaldi, M. (2008). Yield response of corn to irrigation and nitrogen fertilization in a Mediterranean environment. *Field Crops Research*, *105*(3), 202–210. https://doi.org/10.1016/j.fcr.2007.10.004

Peñuelas, J., Poulter, B., Sardans, J., Ciais, P., van der Velde, M., Bopp, L., et al. (2013). Human-induced nitrogen–phosphorus imbalances alter natural and managed ecosystems across the globe. *Nature Communications*, *4*. https://doi.org/10.1038/ncomms3934

Portmann, F. T., Siebert, S., & Döll, P. (2010). MIRCA2000-Global monthly irrigated and rainfed crop areas around the year 2000: A new high-resolution data set for agricultural and hydrological modeling: monthly irrigated and rainfed crop areas. *Global Biogeochemical Cycles*, *24*(1), n/a-n/a. https://doi.org/10.1029/2008GB003435

Pradhan, P., Fischer, G., van Velthuizen, H., Reusser, D. E., & Kropp, J. P. (2015). Closing Yield Gaps: How Sustainable Can We Be? *PLOS ONE*, *10*(6), e0129487. https://doi.org/10.1371/journal.pone.0129487

Ramankutty, N., Evan, A. T., Monfreda, C., & Foley, J. A. (2008). Farming the planet: 1. Geographic distribution of global agricultural lands in the year 2000. *Global Biogeochemical Cycles*, *22*(1), n/a-n/a. https://doi.org/10.1029/2007GB002952

Restelatto, R., Menezes, L. F. G. de, Paris, W., Sartor, L. R., Martin, T. N., Herrera, W. F. B., & Pavinato, P. S. (2017). Sorghum and black oat forage production and its nutritive value under phosphate levels. *Semina: Ciências Agrárias*, *38*(1), 429. https://doi.org/10.5433/1679-0359.2017v38n1p429

Ringeval, B., Nowak, B., Nesme, T., Delmas, M., & Pellerin, S. (2014). Contribution of anthropogenic phosphorus to agricultural soil fertility and food production. *Global Biogeochemical Cycles*, *28*(7), 743–756. https://doi.org/10.1002/2014GB004842

Ringeval, B., Augusto, L., Monod, H., van Apeldoorn, D., Bouwman, L., Yang, X., et al. (2017). Phosphorus in agricultural soils: drivers of its distribution at the global scale. *Global Change Biology*. https://doi.org/10.1111/gcb.13618

Ringeval, B., Müller, C., Pugh, T. A. M., Mueller, N. D., Ciais, P., Folberth, C., et al. (2021). Potential yield simulated by global gridded crop models: using a process-based emulator to explain their differences. *Geoscientific Model Development*, *14*(3), 1639–1656. https://doi.org/10.5194/gmd-14-1639-2021

Ringeval, B., 2021, "Global gridded dataset about supply and demand for nitrogen and phosphorus for cereals", https://doi.org/10.15454/NXYH6G, Portail Data INRAE, V2

Ryan, M. H., & Graham, J. H. (2018). Little evidence that farmers should consider abundance or diversity of arbuscular mycorrhizal fungi when managing crops. *New Phytologist*, *220*(4), 1092–1107. https://doi.org/10.1111/nph.15308

Sadras, V. O. (2006). The N:P stoichiometry of cereal, grain legume and oilseed crops. *Field Crops Research*, *95*(1), 13–29. https://doi.org/10.1016/j.fcr.2005.01.020

Salvagiotti, F., Cassman, K. G., Specht, J. E., Walters, D. T., Weiss, A., & Dobermann, A. (2008). Nitrogen uptake, fixation and response to fertilizer N in soybeans: A review. *Field Crops Research*, *108*(1), 1–13. https://doi.org/10.1016/j.fcr.2008.03.001

Sattari, S. Z., Bouwman, A. F., Giller, K. E., & van Ittersum, M. K. (2012). Residual soil phosphorus as the missing piece in the global phosphorus crisis puzzle. *Proceedings of the National Academy of Sciences USA*, *109*(16), 6348–6353. https://doi.org/10.1073/pnas.1113675109

Sattari, S. Z., van Ittersum, M. K., Bouwman, A. F., Smit, A. L., & Janssen, B. H. (2014). Crop yield response to soil fertility and N, P, K inputs in different environments: Testing and improving the QUEFTS model. *Field Crops Research*, *157*, 35–46.

https://doi.org/10.1016/j.fcr.2013.12.005

Schils, R., Olesen, J. E., Kersebaum, K.-C., Rijk, B., Oberforster, M., Kalyada, V., et al. (2018). Cereal yield gaps across Europe. *European Journal of Agronomy*, *101*, 109–120.

Sinclair, T. R., & Park, W. I. (1993). Inadequacy of the Liebig limiting-factor paradigm for explaining varying crop yields. *Agronomy Journal*, *85*(3), 742–746.

Sistla, S. A., & Schimel, J. P. (2012). Stoichiometric flexibility as a regulator of carbon and nutrient cycling in terrestrial ecosystems under change: Research review. *New Phytologist*, *196*(1), 68–78. https://doi.org/10.1111/j.1469-8137.2012.04234.x

Smil, V. (1999). Nitrogen in crop production: an account of global flows. *Global Biogeochemical Cycles*, *13*(2), 647–662. https://doi.org/0886-6236/99/1999GB900015512.00

Trinsoutrot, I., Recous, S., Bentz, B., Linères, M., Chèneby, D., & Nicolardot, B. (2000). Biochemical Quality of Crop Residues and Carbon and Nitrogen Mineralization Kinetics under Nonlimiting Nitrogen Conditions. *Soil Science Society of America Journal*, *64*(3), 918–926. https://doi.org/10.2136/sssaj2000.643918x

De Wit, C. de. (1992). Resource use efficiency in agriculture. *Agricultural Systems*, *40*(1-3), 125–151.

Wang, X., Müller, C., Elliot, J., Mueller, N. D., Ciais, P., Jägermeyr, J., et al. (2021). Global irrigation contribution to wheat and maize yield. *Nature Communications*, *12*(1), 1235. https://doi.org/10.1038/s41467-021-21498-5

Wang, Y., Ying, H., Yin, Y., Zheng, H., & Cui, Z. (2019). Estimating soil nitrate leaching of nitrogen fertilizer from global meta-analysis. Science of The Total Environment, 657, 96–102. https://doi.org/10.1016/j.scitotenv.2018.12.029

Willigen, P. D., & Noordwijk, M. V. (1994). Mass flow and diffusion of nutrients to a root with constant or zero-sink uptake II. Zero-sink uptake. Soil Science, pp. 171–175.

Yue, K., Fornara, D. A., Yang, W., Peng, Y., Peng, C., Liu, Z., & Wu, F. (2017). Influence of multiple global change drivers on terrestrial carbon storage: additive effects are common. Ecology Letters, 20(5), 663–672. https://doi.org/10.1111/ele.12767

Zaehle, S., & Dalmonech, D. (2011). Carbon–nitrogen interactions on land at global scales: current understanding in modelling climate biosphere feedbacks. *Current Opinion in Environmental Sustainability*, *3*(5), 311–320. https://doi.org/10.1016/j.cosust.2011.08.008

Tables

Table 1 (two pages). Nutrient limitation categories defined in Harpole et al. (2011) and for each category, theoretical conditions required for R_N and R_P to make an ecosystem in this category and its occurrence at the global scale for maize. Columns 1, 3, 4 define each category and are based on Harpole et al. (2011). Columns 5 and 7 give the conditions in terms of R_N and R_P (i.e. the limitations in the control experiment) required to be in each category. This is the result of our theoretical framework. Columns 6 and 8 give the occurrence of each category for maize at the global scale and are the results of our modeling approach. Both results of the theoretical framework and modeling approach are given for two formalisms of interaction: multiple limitation hypothesis (MH, columns 5 and 6) and Liebig's law of minimum (LM, columns 7 and 8).

Long name of the category	Letter used hereafter to name the category	Definition of the category based on the changes in productivity following addition of N alone (red dot, Δpro_{+N}) , P alone (blue dot, Δpro_{+P}) and NP (magenta dot, Δpro_{+NP}) from the control (white dot). Legend: ○ Ctrl 🔴 +N 🔵 +P 🟣 +NP	Does this category correspond to co-limitation? If yes, what kind of co-limitation?	Theoretical conditions required to be in that category for MH **	Occurrence for MH: in percent of global maize area (or in percent of grid-cells within brackets)	Theoretical conditions required to be in that category for LM	Occurrence for LM: in percent of global maize area (or in percent of grid-cells within brackets)
Simultaneous co-limitation	A	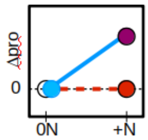 $\Delta\, pro_{+N}=0$ $\Delta\, pro_{+P}=0$ $\Delta\, pro_{+NP}>\Delta\, pro_{+N}+\Delta\, pro_{+P}$	Co-limitation: true and synergistic	$R_N=0$ and $R_P=0$	0.0±0.0 (0.0±0.0)	$R_P=R_N\neq 1$	0.0±0.0 (0.0±0.0)
Independent co-limitation; super-additive *	B	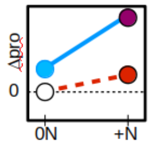 $\Delta\, pro_{+N}\neq 0$ $\Delta\, pro_{+P}\neq 0$ $\Delta\, pro_{+NP}>\Delta\, pro_{+N}+\Delta\, pro_{+P}$	Co-limitation: true and synergistic	R_N in (0,1) and R_P in (0,1)	38.2±0.6 (34.8±0.3)	Cannot occur	0.0±0.0 (0.0±0.0)
Serial limitation N	C	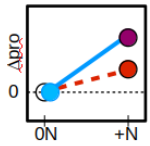 $\Delta\, pro_{+N}\neq 0$ $\Delta\, pro_{+P}=0$ $\Delta\, pro_{+NP}>\Delta\, pro_{+N}+\Delta\, pro_{+P}$	Co-limitation: synergistic	$R_N=0$ and R_P in (0,1)	7.2±0.3 (9.7±0.2)	$R_N<R_P$ and $R_P(E_2)<R_N(E_2)$ ***	5.7±0.4 (9.2±0.3)
Serial limitation P	D	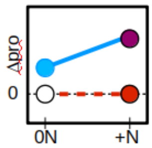 $\Delta\, pro_{+N}=0$ $\Delta\, pro_{+P}\neq 0$ $\Delta\, pro_{+NP}>\Delta\, pro_{+N}+\Delta\, pro_{+P}$	Co-limitation; synergistic	R_N in (0,1) and $R_P=0$	0.0±0.0 (0.0±0.0)	$R_P<R_N$ and $R_N(E_3)<R_P(E_3)$	7.1±0.5 (9.4±0.3)

Single-resource response N	E	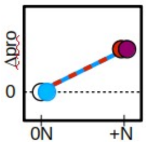 $\Delta pro_{+N} \neq 0$ $\Delta pro_{+P} = 0$ $\Delta pro_{+NP} = \Delta pro_{+N} + \Delta pro_{+P}$	No co-limitation	R_N in [0,1) and $R_P=1$	31.2±0.6 (40.7±0.4)	$R_N<R_P$ and $R_P(E_2)\geq R_N(E_2)$ ****	40.3±0.7 (53.2±0.5)
Single-resource response P	F	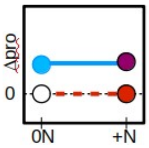 $\Delta pro_{+N} = 0$ $\Delta pro_{+P} \neq 0$ $\Delta pro_{+NP} = \Delta pro_{+N} + \Delta pro_{+P}$	No co-limitation	$R_N=1$ and R_P in [0,1)	7.5±0.5 (3.6±0.1)	$R_P<R_N$ and $R_N(E_3)\geq R_P(E_3)$	31.1±0.8 (17.1±0.5)
No response	G	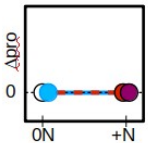 $\Delta pro_{+N} = 0$ $\Delta pro_{+P} = 0$ $\Delta pro_{+NP} = \Delta pro_{+N} + \Delta pro_{+P}$	No co-limitation	$R_N=1$ and $R_P=1$	15.8±0.4 (11.1±0.2)	$R_N=1$ and $R_P=1$	15.8±0.4 (11.1±0.2)

** the category B is restricted in this study to synergistic cases (called "super-additive" in Harpole et al. 2011) while non-synergistic cases (called "sub-additive" or "additive" in Harpole et al. 2011) can happen. Such non-synergistic co-limitations are allowed neither by MH nor by LM (Text S1).*

*** a parenthesis instead of a square bracket used in an interval means that the corresponding endpoint is excluded from the interval; e.g. R in [0,1) means 0≤R<1.*

**** corresponds to "E_1: N-limited and E_2: P-limited"*

***** corresponds to "E_1: N-limited and (E_2: N-limited or NP-limited or not limited at all)"*

Table 2: Summary of the computation of supply and demand in N and P

Variable	Name	Unit	Computation	Source of data	For any grid-cell, computation of one replicate among 1000 ones computed to consider uncertainty	Crop dependence (wheat, maize, rice) ?	More details in	Reference of the computation
S_P	P supply	kgP/ha/yr	$S_P = \sum_{j=1,12} (A_{root}(j).P_{uptake}(j)) + \alpha.P_{fert}/CI$ with *j* : month, A_{root} : monthly root area per unit soil surface area (m^2/ha), P_{uptake}: monthly potential P root uptake per unit root surface area ($kgP/m^2/month$), α: a constant (-), P_{fert}: inorganic content of total P fertilizer applied the year considered (kgP/ha/yr), CI: crop harvest per year (-).	A_{root}, P_{uptake} : Kvakić et al. (2018) P_{fert}: Ringeval et al. (2017) CI: Portmann et al., (2010) α: constant value at the global scale	Through a combination of: - A_{root}, P_{uptake} : one value among 1000 replicates given by Kvakić et al. (2018) - P_{fert}: one value among 30 replicates given by Ringeval et al. (2017) - α: one random value within a normal distribution with average=0.17 and CV=20%	Yes, through: - A_{root} - P_{uptake} that depends on root biomass (the soil P maps (Bruno Ringeval et al., 2017) are not crop-dependent) - CI	Text S3	(Kvakić et al., 2018)
D_P	P demand	kgP/ha/yr	$D_P = Y_{pot}.(\frac{P_{\%,grain}}{PHI} + \frac{P_{\%,root}.RSR}{HI})$ with Y_{pot}: potential yield (kgC/ha/yr), PHI: P harvest index (-), HI: harvest index (-), RSR: root:shoot ratio (-) and $P_{\%,grain}$ and $P_{\%,root}$: P concentration for grain and root, respectively (kgP/kgC).	Y_{pot}: Mueller et al. (2012) PHI, HI, RSR, $P_{\%,grain}$, $P_{\%,root}$: constant values at the global scale derived from the literature	One random value within a normal distribution for each parameters (PHI, HI, RSR, $P_{\%,grain}$, $P_{\%,root}$) with average and STD provided in the literature	Yes	Text S2 and Table S1	(Kvakić et al., 2018)
S_N	N supply	kgN/ha/yr	$S_N = N_{fix} + N_{dep} + N_{fert} + N_{man} + N_{res} - N_{vol} - N_{leach}$ with N_{fix}, N_{dep}, N_{fert}, N_{man}, N_{res}: soil N input corresponding to symbiotic fixation, atmospheric deposition, chemical fertilizer, manure applied on cropland soil, and crop residues remaining on/within	N_{fix}, N_{dep}, N_{fert}, $N_{man,}$ N_{vol}: derived from Bouwman et al. (2011) (average among different categories: extensive/intensive or	One random value within a normal distribution with CV=20% assumed (20% corresponds to the default value of uncertainty in Kvakić et al. (2018)	No	Text S4	(L. Bouwman et al., 2011b) (Hergou

			the cropland soil, respectively (kgN/ha/yr); and N_{vol} and N_{leach} : soil output corresponding to NH_3 volatilization and leaching (kgN/ha/yr).	upland/rice/ leguminous) N_{res}: derived from N in harvest given by Bouwman et al. (2011) and global parameters based on Smil (1999). N_{leach}: computed following the IPCC (Hergoualc'h, 2019)				alc'h, 2019)
D_N	N demand	kgN/ha/yr	$D_N = Y_{pot} . (\frac{N_{\%,grain}}{NHI} + \frac{N_{\%,root} . RSR}{HI})$ with Y_{pot}: potential yield (kgC/ha/yr), NHI: N harvest index (-), HI: harvest index (-), RSR: root:shoot ratio (-) and $N_{\%,grain}$ and $N_{\%,root}$: N concentration for grain and root, respectively (kgN/kgC).	Y_{pot}: Mueller et al. (2012) NHI, HI, RSR, $N_{\%,grain}$, $N_{\%,root}$: constant values at the global scale derived from the literature	One random value within a normal distribution for each parameters (NHI, HI, RSR, $N_{\%,grain}$, $N_{\%,root}$) with average and STD provided in the literature	Yes	Text S2 and Table S1	This study

Table 3. Global values (± one standard-deviation) of the supply/demand ratio (R) for N, P or NP. The ratio R_{NP} is given for the two formalims of interaction: multiple limitation hypothesis (MH) and Liebig's law of minimum (LM).

Nutrient(s)		N	P	NP (formalism MH)	NP (formalism LM)
Ratio (R)	Maize	0.52 ± 0.00	0.61 ± 0.01	0.34 ± 0.00	0.37 ± 0.01
	Wheat	0.60 ± 0.00	0.72 ± 0.01	0.47 ± 0.00	0.49 ± 0.00
	Rice	0.77± 0.00	0.77 ± 0.01	0.62 ± 0.01	0.63 ± 0.01

Figures

Figure 1. Schematic representation of the fertilization experiments. The different experiments (called E_1-E_4) vary as function of their supply of N (S_N or S_N+A_N) and P (S_P or S_P+A_P) with S_X: soil supply in the CTRL experiment and A_X: increase in soil supply following the addition of fertilizer, for the nutrient X with X in {N,P}. For a given nutrient X, D_X is the demand in this nutrient and is similar in all experiments.

Figure 2. R_{NP}, ΔR_N and ΔR_P for any values of R_N (x-axis) and R_P (y-axis). ΔR_N and ΔR_P corresponds to change in R_N and R_P required at the same time to make R_{NP} equal to 0.75. Each variable is provided for the two formalisms of interaction (LM – 1st line - and MH - 2nd line) as well as for the difference LM-MH (last line). Note that the colorbar was inverted in panels d,e,g,h to show large values of ΔR_N and ΔR_P in red. White area in each panel correspond to values between 0 and 0.001. Grey transparent dots in panels c,f,i correspond to all grid-cells considered for maize in our modelling approach.

Figure 3. Schematic representation of the computation of (ΔR_N, ΔR_P). A given grid-cell is defined by its (R_N, R_P) in the plan characterized by the base $(\vec{R}_N, \vec{R}_P)$. For a given grid-cell and a given formalism, we called $\vec{u}$ the shortest vector linking (R_N, R_P) and the curve (or segments) defining R_{NP}=0.75. We called x and y the compounds of $\vec{u}$ in the base $(\vec{R}_N, \vec{R}_P)$, i.e. $\vec{u} = \begin{pmatrix} x \\ y \end{pmatrix}$. We defined $\Delta R_N = max(0, x)$ and $\Delta R_P = max(0, y)$. In the above figure, two grid-cells are provided as an example: (R_N=0.2; R_P=0.5) for the black dot, and (R_N=0.9; R_P=0.1) for the black star. The formalism of interaction defines the (R_N,R_P) couples that make R_{NP}=0.75: the blue curve defines R_{NP}=0.75 for MH while the two orthogonal red segments define R_{NP}=0.75 for LM. $\vec{u}$ is provided for each grid-cell and each formalism (blue arrow for MH ; red arrow for LM). We explicitly plotted the ΔR_N and ΔR_P for the black dot and the two formalisms (solid black lines). Note that for the grid-cell symbolized by the black star, $\Delta R_N = 0$ for LM.

Figure 4. Spatial distribution of the categories defined in Table 1 and in Harpole et al. (2011) for multiple limitation hypothesis (MH, panel a) and Liebig's law of minimum (LM, b) for maize. Category A corresponds to simultaneous co-limitation, category B to independent co-limitation (super-additive), categories C and D to serial limitation (N and P, respectively), categories E and F to single-resource response (N and P, respectively) and category G to no response. The same color (but with different shades: light and dark) has been chosen for the different categories within each co-limitation type: true and synergistic co-limitation (blue), synergistic co-limitation (red) and no co-limitation (green). For LM, whether one grid-cell belongs either to category C (light red) or to category E (light green) depends on the increase in soil N supply following the N fertilizer addition in the fertilizing experiment (called A_N in Eq.3-6). The same reasoning applies for categories D (dark red) and F (dark green) with the increase in soil P supply following the addition of P fertilizer (A_P in Eq.3-6).

Data and Code availability:

Files corresponding to supply and demand for N and P (variables called S_N, S_P, D_N, D_P in the manuscript) are made available (Ringeval et al., 2021) on the following link: https://doi.org/10.15454/NXYH6G. Computer scripts written by the authors to generate and manipulate files of supply and demand for N and P are available upon request to the corresponding author.

Acknowledgements:

This research was supported by the “Institut National de Recherche pour l'agriculture, l'alimentation et l'environnement” (INRAE) and the AgroEcoSystem division. We thank Lex Bouwman for providing variables at the basis of N supply computation. We thank Thomas A.M. Pugh, Frédéric Barraquand, Alain Mollier, Pascal Denoroy, Pietro Barbieri, Mark Irvine, Tovo Rabemanantsoa and Noémie Schaller for helpful discussion. Finally, we would like to thank Aldyth Nys for her assistance with the linguistic aspects of this paper. Modelling and analysis were performed in using Python (Python Software Foundation. Python Language Reference, version 2.7. Available at http://www.python.org).

Author contribution:

B.R conceived the project; B.R. and M.K. performed the computations; B.R, S.P and L.A analysed the results; N.D.M, C.M, T.A.M.P and X.W. provided datasets and their expertise on these datasets; B.R, M.K, L.A, P.C, D.G, N.D.M, C.M, T.N, T.A.M.P, N.V, S.P wrote the article.

Competing interests:

The authors declare no conflict of interest.

Supporting Information

Supporting Text

Text S1. Analytical characterization of the categories defined in Harpole et al. (2011)
Text S2. Computation of the nutrient demand (D_N and D_P)
Text S3. Computation of the supply of P (S_P)
Text S4. Computation of N in residues remaining on cropland soil (N_{res})
Text S5. Spatial distribution of R_N, R_P, R_{NP}
Text S6. Relationship between R_{NP} and yield gap

Supporting Figures

Figure S1. Spatial distribution of ΔR_N and ΔR_P
Figure S2. The effect of using the actual yield (instead of potential yield) on the computed nutrient limitation
Figure S3. Grid-cell distribution in percentiles of different variables
Figure S4. For maize, spatial distribution of R_N and R_P when N and P are considered as independent: average and standard-deviation of the 1000 replicates
Figure S5. For maize, the spatial distribution of nutrient limitation when N and P are considered to be independent (bivariate plot of R_N and R_P)
Figure S6. For maize, spatial distribution of $\mathrm{R_{NP}}$: average and standard-deviation for both formalisms of interaction
Figure S7. Scatterplots of the ratio Y_{real}/Y_{pot} provided by Mueller et al. (2012) vs. the simulated R_{NP} at the country scale for maize

Supporting Tables

Table S1. Parameters used to estimate the N and P demands (D_N and D_P, respectively)
Table S2. Global crop area and production provided by global datasets and considered in our study
Table S3. For all crops, global values of supply (S), demand (D) and supply/demand ratio (R) for N and P when the two nutrients are considered as independent

Figure 1

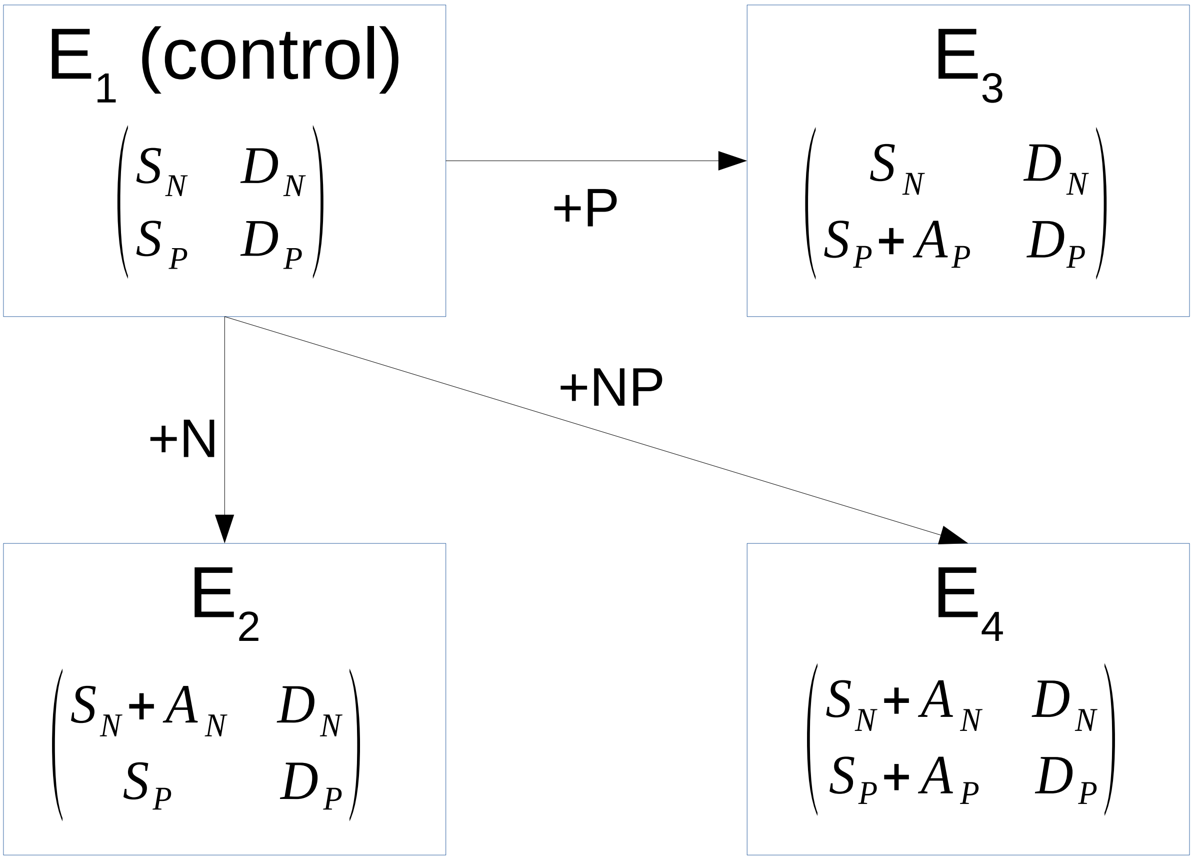
E_1 (control)
$\begin{pmatrix} S_N & D_N \\ S_P & D_P \end{pmatrix}$
+P
E_3
$\begin{pmatrix} S_N & D_N \\ S_P+A_P & D_P \end{pmatrix}$
+NP
+N
E_2
$\begin{pmatrix} S_N+A_N & D_N \\ S_P & D_P \end{pmatrix}$
E_4
$\begin{pmatrix} S_N+A_N & D_N \\ S_P+A_P & D_P \end{pmatrix}$

Figure 2

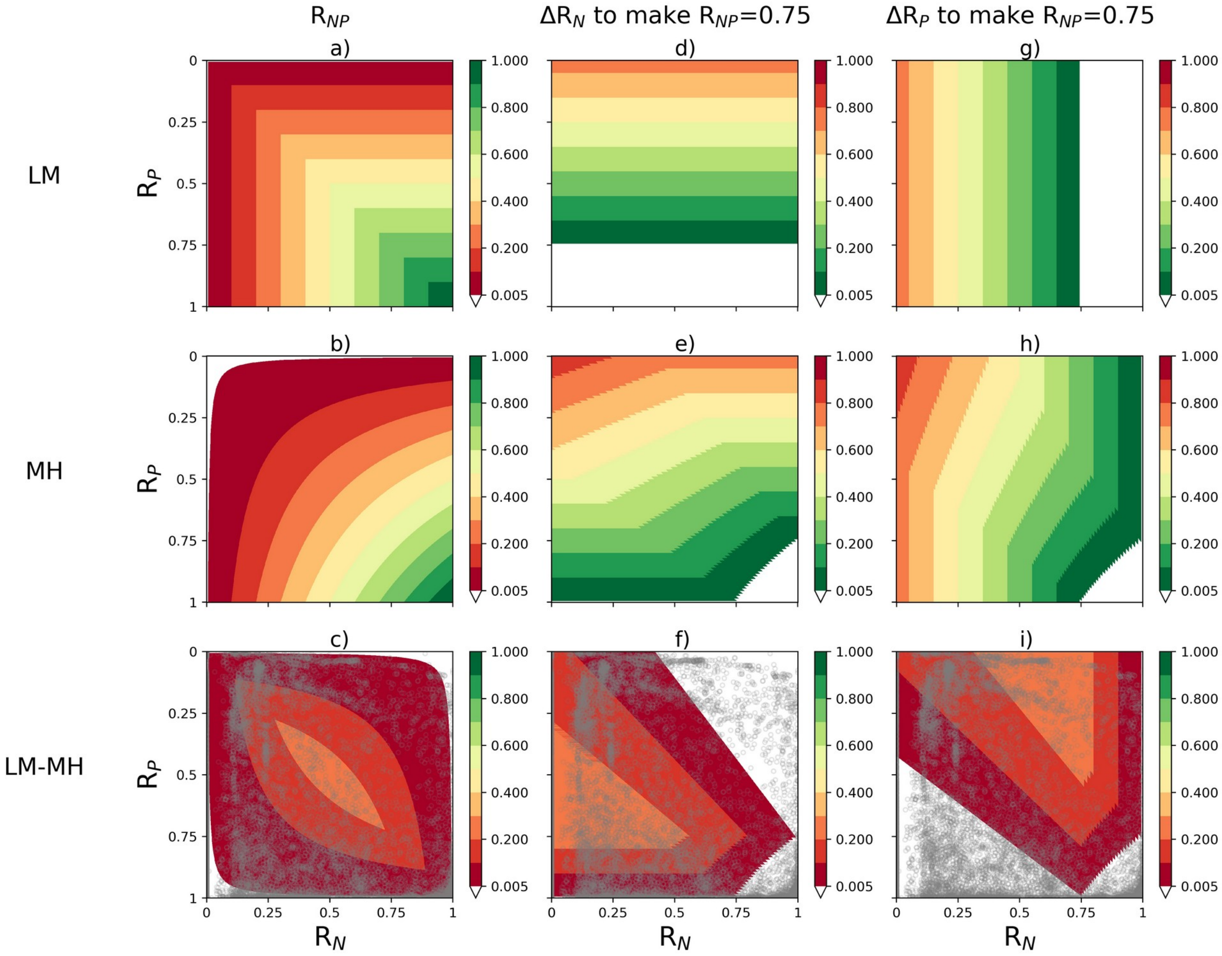
R$_{NP}$
ΔR$_N$ to make R$_{NP}$=0.75
ΔR$_P$ to make R$_{NP}$=0.75
a)
b)
c)
d)
e)
f)
g)
h)
i)
LM
MH
LM-MH
R$_P$
R$_N$
0
0.25
0.5
0.75
1
1.000
0.800
0.600
0.400
0.200
0.005

Figure 3

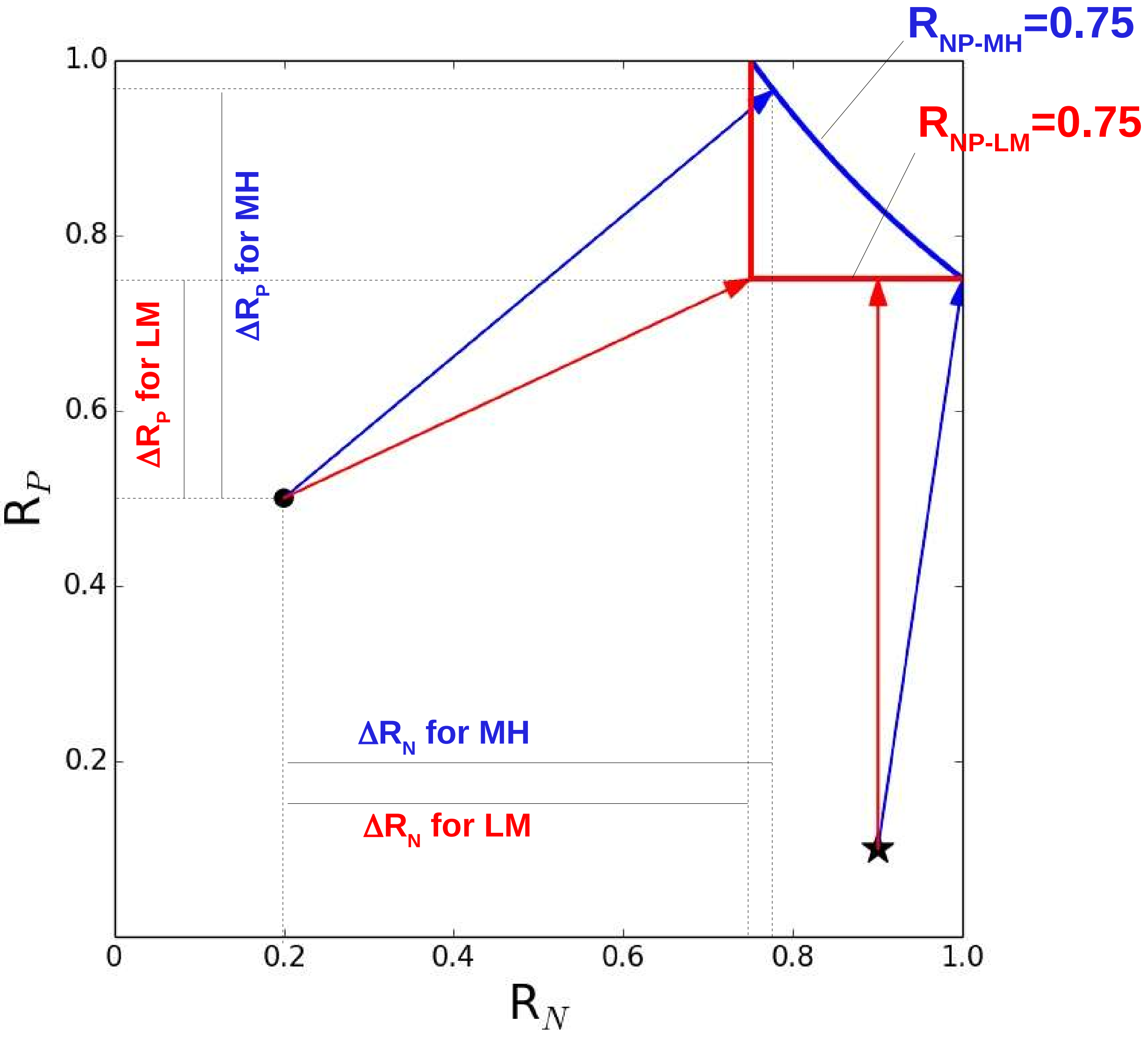
R$_{NP-MH}$=0.75
R$_{NP-LM}$=0.75
ΔR$_P$ for MH
ΔR$_P$ for LM
ΔR$_N$ for MH
ΔR$_N$ for LM
1.0
0.8
0.6
0.4
0.2
0
0.2
0.4
0.6
0.8
1.0
R$_P$
R$_N$

Figure 4

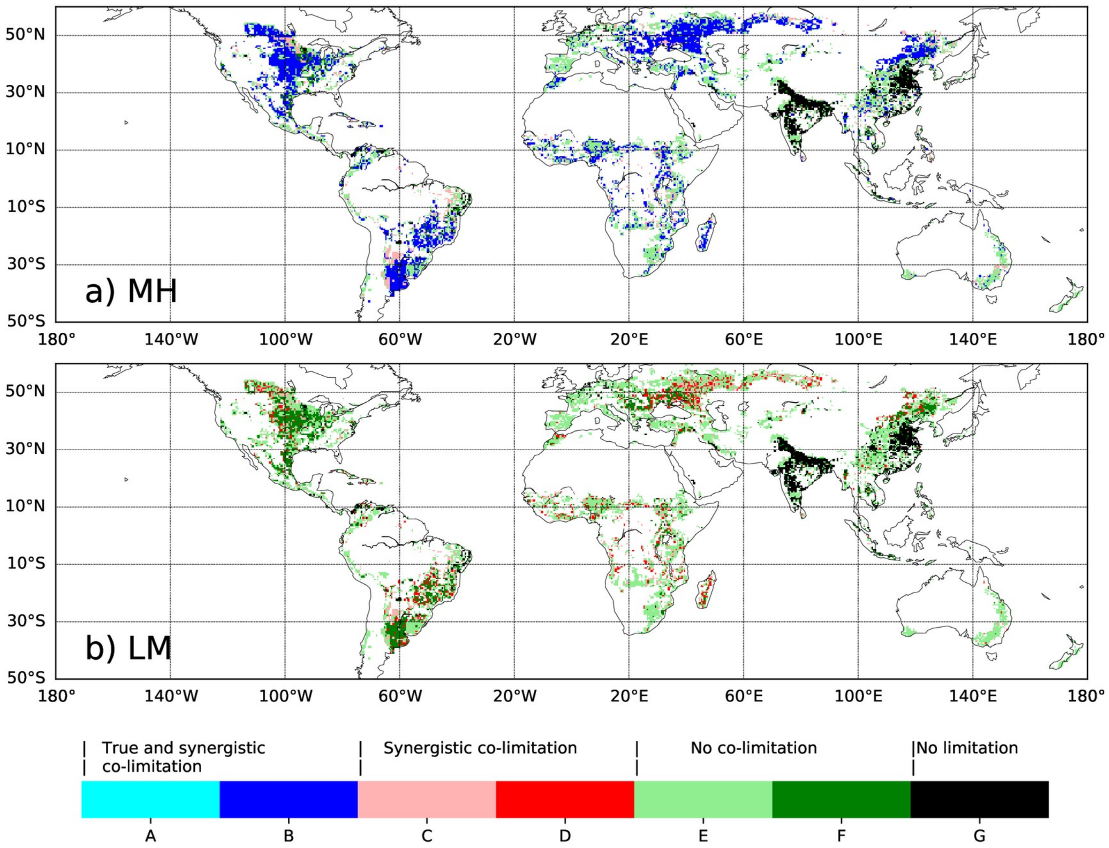
a) MH
b) LM
50°N
30°N
10°N
10°S
30°S
50°S
180°
140°W
100°W
60°W
20°W
20°E
60°E
100°E
140°E
180°
True and synergistic co-limitation
Synergistic co-limitation
No co-limitation
No limitation
A
B
C
D
E
F
G

AGU PUBLICATIONS

Global Biogeochemical Cycles

Supporting Information for

Insights on nitrogen and phosphorus co-limitation in global croplands from theoretical and modelling fertilization experiments

Bruno Ringeval[1]*, Marko Kvakić[1,2], Laurent Augusto[1], Philippe Ciais[2], Daniel Goll[2], Nathaniel D. Mueller[3,4], Christoph Müller[5], Thomas Nesme[1], Nicolas Vuichard[2], Xuhui Wang[6], Sylvain Pellerin[1]

1 : ISPA, Bordeaux Sciences Agro, INRAE, 33140, Villenave d'Ornon, France.
2 : Laboratoire de Sciences du Climat et de l'Environnement, LSCE/IPSL, CEA-CNRS-UVSQ, Universite Paris-Saclay, Gif-sur-Yvette, France
3 : Department of Ecosystem Science and Sustainability, Colorado State University, Fort Collins, CO, USA
4: Department of Soil and Crop Sciences, Colorado State University, Fort Collins, CO, USA
5 : Potsdam Institute for Climate Impact Research, Member of the Leibniz Association, Potsdam, Germany
6: Sino-French Institute of Earth System Sciences, Peking University, 100871 Beijing, China.

Content of this file

Text S1 to S6
Figures S1 to S7
Tables S1 to S3

Introduction

The supplementary information gives further details on the following methods:

- an analytical characterization of the categories defined in Harpole et al. (2011) (Text S1)
- computation of N and P demands, P supply and one term within N supply computation (Text S2-S4)

as well as extended description of results:

- description of the spatial distribution of R_N, R_P, R_{NP} and relationship between this later and yield gap (Text S6-S7)

Additionally, figures corresponding to extended results are provided. Tables of numerical values used in various methodological steps or of extended results are also given. Figures and tables are referred to either in the Supp.Inf or in the main text.

Text S1. Analytical characterization of the categories defined in Harpole et al. (2011).

We characterized the limitation of a nutrient considered alone as the variable *R* which is a function of the ratio between its soil supply (*S*) and the demand by the plant to achieve its potential biomass (*D*): $R_N = f(\frac{S_N}{D_N})$ and $R_P = g(\frac{S_P}{D_P})$ with S_N: the supply in N, S_P: the supply in P, D_N: the demand in N and D_P: the demand in P, all in kg (N or P)/ha/yr; and *f* and *g* are mathematical functions. Analytical investigations performed below are valid for any functions *f* and *g* that satisfy the following conditions:

- *f (0)=0* and *g(0)=0*; and
- *f* and *g* are growing over [0,+inf[and are strictly growing over [0,*thresh*] with *thresh*≤1.

The analytical analysis performed below are done with two formalisms of interaction: multiple limitation hypothesis (called MH) or Liebig's law of the minimum (LM). With LM, the analysis below requires *f=g* to be valid while *f* and *g* can be different with MH. From now, and for the sake of simplicity, we choose *f=g* for both MH and LM. We also use as simple function as possible for *f*. Thus, we defined the mathematical function *f* as: $f(x) = min(1, x)$ with *x* varying within [0,+inf[. Thus, $R_N = f(\frac{S_N}{D_N}) = min(1, \frac{S_N}{D_N})$ and $R_P = f(\frac{S_P}{D_P}) = min(\frac{S_P}{D_P})$. The variable R_X (with X in {N,P}) varies in [0,1]. R_X cannot be greater than 1 as we studied limitation that cannot happen when the supply is greater to the demand. R_X close to 0 means a very high limitation while R_X close to 1 means no limitation. For any ratio S_X/D_X varying between 0 and 1, R_X is equal to this ratio.

Crossed fertilization experiments are a common tool to assess nutrient limitation on a given site. They correspond to changes in nutrient supply in different combinations from the control (E_1): addition of N alone (E_2), P alone (E_3) or N and P together (E_4). Based on the above equations defining the limitations of N and P, theses changes in nutrient supply translate into limitations of each nutrient for each experiment E as follows:

E_1: $R_N(E_1) = f(\frac{S_N}{D_N})$ and $R_P(E_1) = f(\frac{S_P}{D_P})$ (Eq.S1)

E_2: $R_N(E_2) = f(\frac{S_N + A_N}{D_N})$ and $R_P(E_2) = f(\frac{S_P}{D_P})$ (Eq.S2)

E_3: $R_N(E_3) = f(\frac{S_N}{D_N})$ and $R_P(E_3) = f(\frac{S_P + A_P}{D_P})$ (Eq.S3)

E_4: $R_N(E_4) = f(\frac{S_N + A_N}{D_N})$ and $R_P(E_4) = f(\frac{S_P + A_P}{D_P})$ (Eq.S4)

with A_N and A_P corresponding to the increase of N and P soil supply following addition of N and P, respectively. $R_N(E_1)$ and $R_P(E_1)$ are called R_N and R_P, respectively.

Two formalisms of interaction have been here considered to compute R_{NP} from R_N and R_P: multiple limitation hypothesis (called MH) or Liebig's law of the minimum (LM):

$R_{NP\_MH}(E_i) = R_N(E_i) * R_P(E_i)$ (Eq.S5)

$R_{NP\_LM}(E_i) = min(R_N(E_i), R_P(E_i))$ (Eq.S6)

where E_i is the experiment *i*, with *i* in {1,2,3,4}.

We assumed that the change in productivity (*Δpro*) following the addition of +N, +P or +NP is equal to the change in R_{NP} following the nutrient addition, i.e.:

$\Delta pro_{+N}=R_{NP}(E_2)-R_{NP}(E_1)$ (Eq.S7)

$\Delta pro_{+P}=R_{NP}(E_3)-R_{NP}(E_1)$ (Eq.S8)

$\Delta pro_{+NP}=R_{NP}(E_4)-R_{NP}(E_1)$ (Eq.S9).

As shown in the column 3 of Table 1, each category of Harpole et al. (2011) could be defined as a combination of following properties: ($\Delta pro_{+N}\neq 0$ or $\Delta pro_{+N}=0$) AND ($\Delta pro_{+P}\neq 0$ or $\Delta pro_{+P}=0$) AND ($\Delta pro_{+NP}>\Delta pro_{+N}+\Delta pro_{+P}$ or $\Delta pro_{+NP}=\Delta pro_{+N}+\Delta pro_{+P}$). In the following, we manipulated the equations (Eq.S1-S9) to translate these properties within implications for nutrient limitations in the control, i.e. R_N and R_P. This allowed us to translate each definition of the Harpole category in terms of R_N and R_P. This was done for MH (Text S1.1) and LM (Text S1.2) formalisms. Results are summarized in the column 5 of Table 1 for MH and in the column 7 of the same Table for LM.

Preamble

As the function *f* is growing over [0,+inf[, we have :

$$f\left(\frac{S_X+A_X}{D_X}\right)\geq f\left(\frac{S_X}{D_X}\right) \quad \text{(Eq.S10)}$$

with X=N or P. Because we considered A_x as positive and non-null (i.e. in the fertilization experiment of a given element, the supply of this element is increased), the equality $f\left(\frac{S_X+A_X}{D_X}\right)=f\left(\frac{S_X}{D_X}\right)$ is only possible when $f\left(\frac{S_X}{D_X}\right)=1$, i.e. R_X=1. Otherwise, $f\left(\frac{S_X+A_X}{D_X}\right)>f\left(\frac{S_X}{D_X}\right)$. Thus, we have the two equivalences below:

$$\left(f\left(\frac{S_X+A_X}{D_X}\right)>f\left(\frac{S_X}{D_X}\right)\right)\Leftrightarrow(R_X\neq 1) \quad \text{(Ev.S1)}$$

$$\left(f\left(\frac{S_X+A_X}{D_X}\right)=f\left(\frac{S_X}{D_X}\right)=1\right)\Leftrightarrow(R_X=1) \quad \text{(Ev.S2)}$$

Text S1.1. MH formalism

Text S1.1.1. What do $\Delta pro_{+N}\neq 0$, $\Delta pro_{+N}=0$, $\Delta pro_{+P}\neq 0$, $\Delta pro_{+P}=0$, $\Delta pro_{+NP}>\Delta pro_{+N}+\Delta pro_{+P}$ and $\Delta pro_{+NP}=\Delta pro_{+N}+\Delta pro_{+P}$ imply for R$_N$ and R$_P$ values in case of MH formalism?

With MH formalism (i.e. with Eq.S5), the change in productivity (Eq.S7-S9) become:

$$\Delta pro_{+N}=f\left(\frac{S_N+A_N}{D_N}\right).f\left(\frac{S_P}{D_P}\right)-f\left(\frac{S_N}{D_N}\right).f\left(\frac{S_P}{D_P}\right) \quad \text{(Eq.S11)}$$

$$\Delta pro_{+P}=f\left(\frac{S_N}{D_N}\right).f\left(\frac{S_P+A_P}{D_P}\right)-f\left(\frac{S_N}{D_N}\right).f\left(\frac{S_P}{D_P}\right) \quad \text{(Eq.S12)}$$

$$\Delta pro_{+NP}=f(\frac{S_N+A_N}{D_N}).f(\frac{S_P+A_P}{D_P})-f(\frac{S_N}{D_N}).f(\frac{S_P}{D_P})$$ (Eq.S13).

Thanks to Eq.S11, we find that $\Delta pro_{+N}=0$ is only possible if either $f(\frac{S_P}{D_P})=0$ or $f(\frac{S_N+A_N}{D_N})=f(\frac{S_N}{D_N})$. The first condition corresponds to *R*$_P$=0, the 2nd one to *R*$_N$=1 (see Ev.S2). Thus,

$$(\Delta pro_{+N}=0)\Leftrightarrow(R_P=0 \text{ or } R_N=1)$$ (Ev.S3)

And similarly,

$$(\Delta pro_{+P}=0)\Leftrightarrow(R_N=0 \text{ or } R_P=1)$$ (Ev.S4).

Also we have to note that *R*$_N$ (or *R*$_P$) equal to 1 have some implications. From Ev.S2, we have $(R_N=1)\Leftrightarrow(f(\frac{S_N+A_N}{D_N})=f(\frac{S_N}{D_N})=1)$. In that case, Eq.S11-S13 becomes $\Delta pro_{+N}=0$, $\Delta pro_{+P}=f(\frac{S_P+A_P}{D_P})-f(\frac{S_P}{D_P})$ and $\Delta pro_{+NP}=f(\frac{S_P+A_P}{D_P})-f(\frac{S_P}{D_P})$. Thus, we get $\Delta pro_{+NP}=\Delta pro_{+N}+\Delta pro_{+P}$. Thus, $(R_N=1)\Rightarrow(\Delta pro_{+NP}=\Delta pro_{+N}+\Delta pro_{+P})$.
Similarly, $(R_P=1)\Rightarrow(\Delta pro_{+NP}=\Delta pro_{+N}+\Delta pro_{+P})$.

We can then demonstrate that $(\Delta pro_{+NP}=\Delta pro_{+N}+\Delta pro_{+P})\Rightarrow(R_P=1 \text{ or } R_N=1)$ by contraposition as follows. Because of Ev.S1, $\begin{cases}R_N\neq 1\\ R_P\neq 1\end{cases}\Rightarrow\begin{cases}f(\frac{S_N+A_N}{D_N})-f(\frac{S_N}{D_N})>0\\ f(\frac{S_P+A_P}{D_P})-f(\frac{S_P}{D_P})>0\end{cases}$. Thus, $\begin{cases}R_N\neq 1\\ R_P\neq 1\end{cases}\Rightarrow[f(\frac{S_N+A_N}{D_N})-f(\frac{S_N}{D_N})].[f(\frac{S_P+A_P}{D_P})-f(\frac{S_P}{D_P})]>0$. By rearranging, we have $\begin{cases}R_N\neq 1\\ R_P\neq 1\end{cases}\Rightarrow f(\frac{S_N+A_N}{D_N}).f(\frac{S_P+A_P}{D_P})>f(\frac{S_N+A_N}{D_N}).f(\frac{S_P}{D_P})+f(\frac{S_P+A_P}{D_P}).f(\frac{S_N}{D_N})-f(\frac{S_N}{D_N}).f(\frac{S_P}{D_P})$. We can subtract $f(\frac{S_N}{D_N}).f(\frac{S_P}{D_P})$ to each member of the 2nd inequality to found:

$$\begin{cases}R_N\neq 1\\ R_P\neq 1\end{cases}\Rightarrow(\Delta pro_{+NP}>\Delta pro_{+N}+\Delta pro_{+P})$$.

Finally, we have: $(R_N=1)\Rightarrow(\Delta pro_{+NP}=\Delta pro_{+N}+\Delta pro_{+P})$,
$(R_P=1)\Rightarrow(\Delta pro_{+NP}=\Delta pro_{+N}+\Delta pro_{+P})$, and
$(\Delta pro_{+NP}=\Delta pro_{+N}+\Delta pro_{+P})\Rightarrow(R_P=1 \text{ or } R_N=1)$.
i.e. we get:

$$(R_P=1 \text{ or } R_N=1)\Leftrightarrow(\Delta pro_{+NP}=\Delta pro_{+N}+\Delta pro_{+P})$$ (Ev.S5).

Text S1.1.2. Definition of each Harpole category in terms of R$_N$ and R$_P$?

The use of Ev.S3-S5 and the definition of the different categories (column 3 in Table 1) allow us to characterize each category in terms of values for R_N and R_P.

Category A is characterized by:
$\Delta pro_{+N}=0$ (x)
$\Delta pro_{+P}=0$ (y)
$\Delta pro_{+NP}>\Delta pro_{+N}+\Delta pro_{+P}$ (z)
According to Ev.S3, $(x)\Leftrightarrow(R_P=0 \text{ or } R_N=1)$. R_N cannot be equal to 1 otherwise $\Delta pro_{+NP}=\Delta pro_{+N}+\Delta pro_{+P}$ through Ev.S5. Similarly, $(y)\Leftrightarrow(R_N=0 \text{ or } R_P=1)$ and R_P cannot be equal to 1 otherwise $\Delta pro_{+NP}=\Delta pro_{+N}+\Delta pro_{+P}$. The only combination possible is: R_P=R_N=0.

Category C is characterized by:
$\Delta pro_{+N}\neq 0$ (x)
$\Delta pro_{+P}=0$ (y)
$\Delta pro_{+NP}>\Delta pro_{+N}+\Delta pro_{+P}$ (z).
$(y)\Leftrightarrow(R_N=0 \text{ or } R_P=1)$ **.** R_P cannot be equal to 1 because of (z). Thus, R_N=0. In addition, R_P cannot be equal to 0 because it would imply $\Delta pro_{+N}=0$ thanks to Ev.S3. Thus, category C occurs if and only if: R_N=0 and R_P in]0,1[. Note that, in the whole manuscript, a parenthesis instead of a square bracket used in an interval means that the corresponding endpoint is excluded from the interval; e.g. R in [0,1) means 0≤R<1.

Similarly, the category D is characterized by: R_P=0 and R_N in]0,1[.

The category E is characterized by:
$\Delta pro_{+N}\neq 0$ (x)
$\Delta pro_{+P}=0$ (y)
$\Delta pro_{+NP}=\Delta pro_{+N}+\Delta pro_{+P}$ (z).
$(z)\Leftrightarrow(R_N=1 \text{ or } R_P=1)$. R_N cannot be equal to 1 otherwise, $\Delta pro_{+N}=0$. Thus, the category E occurs if and only if: R_P=1 and R_N in [0,1[.

Similarly, the category F is characterized by: R_N=1 and R_P in [0,1[.

Category G is characterized by:
$\Delta pro_{+N}=0$ (x)
$\Delta pro_{+P}=0$ (y)
$\Delta pro_{+NP}=\Delta pro_{+N}+\Delta pro_{+P}$ (z).
$(x)\Leftrightarrow(R_P=0 \text{ or } R_N=1)$ and $(y)\Leftrightarrow(R_N=0 \text{ or } R_P=1)$ and $(z)\Leftrightarrow(R_P=1 \text{ or } R_N=1)$. The only combination allowed is: R_P=R_N=1.

Category B is characterized by:
$\Delta pro_{+N}\neq 0$ (x)
$\Delta pro_{+P}\neq 0$ (y)
$\Delta pro_{+NP}>\Delta pro_{+N}+\Delta pro_{+P}$ (z).
It occurs if and only if: both R_P and R_N are in]0,1[.

Note that, in Harpole et al. (2011), category B encompasses different cases: sub-additive, additive and super-additive. Sub-additive and additive cases are not synergistic, i.e. they are characterized by $(\Delta\, pro_{+NP}) \leq (\Delta\, pro_{+N} + \Delta\, pro_{+P})$. With MH formalism, because of Ev.S3, $(\Delta\, pro_{+N} \neq 0)$ as found in category B implies that $(R_P \neq 0 \text{ and } R_N \neq 1)$. Similarly, $(R_N \neq 0 \text{ and } R_P \neq 1)$. Because $(R_P = 1 \text{ or } R_N = 1) \Leftrightarrow (\Delta\, pro_{+NP} = \Delta\, pro_{+N} + \Delta\, pro_{+P})$ (Ev.S5), it means that $(\Delta\, pro_{+NP}) > (\Delta\, pro_{+N} + \Delta\, pro_{+P})$ necessarily happens in category B. Thus, only super-additive cases can be considered in category B with the MH formalism.

Text S1.2. LM formalism

With LM formalism (i.e. with Eq.S6), EqS7-S9 become:

$$\Delta\, pro_{+N} = min[f(\frac{S_N + A_N}{D_N}), f(\frac{S_P}{D_P})] - min[f(\frac{S_N}{D_N}), f(\frac{S_P}{D_P})] \qquad \text{(Eq.S14)}$$

$$\Delta\, pro_{+P} = min[f(\frac{S_N}{D_N}), f(\frac{S_P + A_P}{D_P})] - min[f(\frac{S_N}{D_N}), f(\frac{S_P}{D_P})] \qquad \text{(Eq.S15)}$$

$$\Delta\, pro_{+NP} = min[f(\frac{S_N + A_N}{D_N}), f(\frac{S_P + A_P}{D_P})] - min[f(\frac{S_N}{D_N}), f(\frac{S_P}{D_P})] \qquad \text{(Eq.S16).}$$

The above equations can be solved if we know how the different ratios involved ($\frac{S_N}{D_N}$, $\frac{S_P}{D_P}$, $\frac{S_N + A_N}{D_N}$, $\frac{S_P + A_P}{D_P}$) and 1 are ranked. In the following, we define the conditions in terms of R_N and R_P encountered in the different experiments that are required to be in each category defined by Harpole et al. (2011).

Text S1.2.1. Sub-case 1: categories C and E

In both categories C and E, the ecosystem is N-limited in the control (E_1): adding N leads to an increase in the productivity (from E_1 to E_2). Because adding P does not change the productivity, the ecosystem in E_1 is not P-limited. In fact, except in some very specific cases, the ecosystem is mono nutrient-limited with the LM formalism. As the ecosystem is N limited in the control (E_1), we have $f(\frac{S_N}{D_N}) < f(\frac{S_P}{D_P})$. Because of (Eq.S10) , we also have $f(\frac{S_N}{D_N}) < f(\frac{S_P}{D_P}) \leq f(\frac{S_P + A_P}{D_P})$.

Thus, Eq.S14-S16 become:

$$\Delta\, pro_{+N} = min[f(\frac{S_N + A_N}{D_N}), f(\frac{S_P}{D_P})] - f(\frac{S_N}{D_N}) \qquad \text{(Eq.S17)}$$

$$\Delta\, pro_{+P} = f(\frac{S_N}{D_N}) - f(\frac{S_N}{D_N}) = 0 \qquad \text{(Eq.S18)}$$

$$\Delta\, pro_{+NP} = min[f(\frac{S_N + A_N}{D_N}), f(\frac{S_P + A_P}{D_P})] - f(\frac{S_N}{D_N}) \qquad \text{(Eq.S19).}$$

Eq.S18 means that adding P does not modify the N-limitation and E_3 is also N-limited. To go further and to distinguish categories C and E, we have to consider the different cases of nutrient limitation in E$_2$.

<u>If E$_2$ is N only-limited</u>, we have $f(\frac{S_N+A_N}{D_N})<f(\frac{S_P}{D_P})$. Because of Eq.S10 applied to P, we get $f(\frac{S_N+A_N}{D_N})<f(\frac{S_P}{D_P})\leq f(\frac{S_P+A_P}{D_P})$. Eq.S17&S19 becomes $\Delta pro_{+N}=f(\frac{S_N+A_N}{D_N})-f(\frac{S_N}{D_N})$ and $\Delta pro_{+NP}=f(\frac{S_N+A_N}{D_N})-f(\frac{S_N}{D_N})$. Thus, $\Delta pro_{+NP}=\Delta pro_{+N}+\Delta pro_{+P}$. We are in the case corresponding to category E.

<u>If E$_2$ is only P-limited</u>, we have:

$$f(\frac{S_P}{D_P})<f(\frac{S_N+A_N}{D_N}) \qquad \text{(Eq.S20)}$$

and Eq.S17 becomes:

$$\Delta pro_{+N}=f(\frac{S_P}{D_P})-f(\frac{S_N}{D_N}) \qquad \text{(Eq.S21).}$$

Because E$_2$ is P-limited, we also have $f(\frac{S_P}{D_P})\neq 1$ and thus, following Ev.S1, we have:

$$f(\frac{S_P}{D_P})<f(\frac{S_P+A_P}{D_P}) \qquad \text{(Eq. S22).}$$

To compute Δpro$_{+NP}$, we have to consider the different limitations that could occur in E$_4$. If E$_4$ is only P-limited, we have $f(\frac{S_P+A_P}{D_P})<f(\frac{S_N+A_N}{D_N})$. If E$_4$ is only N-limited, we have $f(\frac{S_N+A_N}{D_N})<f(\frac{S_P+A_P}{D_P})$. If E$_4$ is N and P limited or non-limited, we have $f(\frac{S_N+A_N}{D_N})=f(\frac{S_P+A_P}{D_P})$. In all cases, we can use Eq.S20 or Eq.S22 to show that $min[f(\frac{S_N+A_N}{D_N}),f(\frac{S_P+A_P}{D_P})]>f(\frac{S_P}{D_P})$. Thus, Eq.S19 becomes $\Delta pro_{+NP}>f(\frac{S_P}{D_P})-f(\frac{S_N}{D_N})$, i.e. thanks to Eq.S21, $\Delta pro_{+NP}>\Delta pro_{+N}+\Delta pro_{+P}$. We are in the case corresponding to category C.

<u>If E$_2$ is both N and P-limited</u>, we have

$$f(\frac{S_P}{D_P})=f(\frac{S_N+A_N}{D_N}) \qquad \text{(Eq.S23).}$$

Thus, Eq.S17 becomes e.g. $\Delta pro_{+N}=f(\frac{S_P}{D_P})-f(\frac{S_N}{D_N})$ and Eq.S19 becomes $\Delta pro_{+NP}=min[f(\frac{S_P}{D_P}),f(\frac{S_P+A_P}{D_P})]-f(\frac{S_N}{D_N})$. Because of Eq.S10, the latter equation is equivalent to $\Delta pro_{+NP}=f(\frac{S_P}{D_P})-f(\frac{S_N}{D_N})$ and thus, $\Delta pro_{+NP}=\Delta pro_{+N}+\Delta pro_{+P}$. We are in the case corresponding to category E**.** Note also that, because there is a P limitation in E$_2$, Eq.S22 also applies here. Thanks to Eq.S23, Eq.S22 becomes $f(\frac{S_P+A_P}{D_P})>f(\frac{S_N+A_N}{D_N})$: E$_4$ is necessarily N-limited.

If E_2 is not limited, we have $f(\frac{S_P}{D_P})=f(\frac{S_N+A_N}{D_N})=1$. In that case, because of Eq.S10, we also have $f(\frac{S_P+A_P}{D_P})=1$ (it means that E_4 is not limited). Eq.S17&S19 becomes $\Delta pro_{+N}=1-f(\frac{S_N}{D_N})$ and $\Delta pro_{+NP}=1-f(\frac{S_N}{D_N})$, respectively. Thus, $\Delta pro_{+NP}=\Delta pro_{+N}+\Delta pro_{+P}$. We are in the case corresponding to category E.

To summarize, category C corresponds to: E_1 N-limited and E_2 P-limited, i.e. the addition of N alone (+N) switches the ecosystem from N-limitation to P-limitation. Category E corresponds to E_1 N-limited and E_2 either N-limited or NP-limited or not limited at all. Expressed with equations, we have:

category C <=> [$R_N<R_P$ and $R_P(E_2)<R_N(E_2)$]
category E <=> [$R_N<R_P$ and $R_P(E_2)\geq R_N(E_2)$]

Text S1.2.2. Other sub-cases

The same reasoning applies to categories D (E_1 P-limited and E_3 N-limited) and F (E_1 P-limited and E_3 either P-limited or NP- limited or not limited at all).

Category A is characterized by E_1 both limited by N and P, thus: $R_P=R_N\neq1$.
Category G is characterized by E_1 neither N-limited nor P-limited, thus, $R_P=R_N=1$.

Category B is defined by $\Delta pro_{+N}\neq0$. Thus, E_1 is N-limited, i.e. $R_N\leq R_P$. Because category B is also characterized by $\Delta pro_{+P}\neq0$, E_1 is also P-limited and we have $R_P\leq R_N$. Thus, $R_P=R_N$. This implies that Eq.S14 could be written as :

$$\Delta pro_{+N}=min[f(\frac{S_N+A_N}{D_N}),f(\frac{S_N}{D_N})]-f(\frac{S_N}{D_N}) \quad \text{(Eq.S24).}$$

Because E_1 is limited, $R_N\neq1$. Because of Ev.S1, Eq.S24 becomes $\Delta pro_{+N}=f(\frac{S_N}{D_N})-f(\frac{S_N}{D_N})$. Thus, $\Delta pro_{+N}=0$ which is contrary to the definition of category B: category B cannot occur with LM.

Text S2. Computation of the nutrient demand (D_N and D_P)

As an example, we focus here on the computation of the demand for P (D_P). Similar equations are used for the computation of D_N. The Harvest index (HI, dimensionless), P harvest index (PHI, dimensionless), root:shoot ratio (RSR, dimensionless), P concentration of a plant organ i ($P_{\%,i}$, in gP/gC) and yield (Y, in gC) are defined as follows:

$$HI=\frac{C_{grain}}{C_{shoot}} \quad (1)$$

$$PHI=\frac{P_{grain}}{P_{shoot}} \quad (2)$$

$$RSR=\frac{C_{root}}{C_{shoot}} \quad (3)$$

$$P_{\%,i}=\frac{P_i}{C_i} \quad (4)$$

$$Y=C_{grain} \quad (5)$$

where C_i: the carbon content of organ i (in gC), Pi : the P content of organ i (in gP), and the *shoot* is defined as (*grain + leaf + stem*).

We aimed to estimate the P demand, that is approached by the sum of P in the shoot and P in the root at maturity: $D_P=P_{shoot}+P_{root}$.

By using (2), (4) (applied to i=grain) and (5), we have: $P_{shoot}=P_{\%,grain}\cdot\frac{Y}{PHI}$.

By using (4) (applied to i=root) and (3), we get: $P_{root}=P_{\%,root}.RSR.C_{shoot}$, then: $P_{root}=P_{\%,root}.RSR.\frac{Y}{HI}$ by using (1) and (5).

Finally, we get: $D_P=P_{\%,grain}\cdot\frac{Y}{PHI}+P_{\%,root}.RSR.\frac{Y}{HI}$. Similarly for N, we found: $D_N=N_{\%,grain}\cdot\frac{Y}{NHI}+N_{\%,root}.RSR.\frac{Y}{HI}$. The potential yield (Y_{pot}) is used to compute the potential demands in N and P (D_N and D_P, respectively). These equations correspond to Eq.12 given in the Main Text.

The spatially explicit potential yield (Y_{pot}) for maize, wheat and rice is provided by Mueller et al. (2012) while the constants $P_{\%,grain}$, $P_{\%,root}$, $N_{\%,grain}$, $N_{\%,root}$, RSR, PHI, NHI and HI are found in the literature (see Table S1).

Text S3. Computation of the supply of P (S_P)

The supply of P (S_P, in kgP/ha/yr) corresponds to the sum of a potential root uptake from P remaining in soils and a prescribed fraction of the inorganic content of total P fertilizer applied in the year considered (Kvakić et al., 2018).:

$$S_P = \sum_{j=1,12} \left(A_{root}(j) . P_{uptake}(j)\right) + \alpha . P_{fert} / CI$$

where j is the month, A_{root} is the monthly root area per unit soil surface area (m^2/ha), $P_{utptake}$ is the monthly potential P root uptake per unit root surface area (kgP/m^2/month), α is constant, P_{fert} is the inorganic content of total P fertilizer applied the year considered (kgP/ha/yr), and CI is crop harvest per year (unitless). As in Kvakić et al. (2018), we assumed that a fraction (α) of the applied fertilizer P is directly available to the plant in the same growing season, thus bypassing the P diffusion pathway. A value of 0.17 is used for α (with an uncertainty of 20%). P_{fert} is determined in (Ringeval et al., 2017) from (Bouwman et al., 2011) datasets and CI is given by (Portmann et al., 2010).

The monthly root area per unit soil surface area (m^2/ha) is computed as follows:

$$A_{root}(j) = (2\pi . R_0 . L_{rv}(j) . \Delta z) . 1e^4$$

with R_0 is the root radius (m), L_{rv} is the root length density (m/m^3) and $1e^4$ allows the unit conversion to square meter per hectar. R_0 of 0.42 (wheat), 0.28 (maize) and 0.23 10^{-3}m (rice) have been used. The computation of L_{rv} is described at the end of the current section.

Following the assumption that the solute concentration at the root surface reaches zero and the uptake of this solute is the same as the rate at which it diffuses there (the so-called "zero-sink" assumption (Willigen and Noordwijk, 1994)), the potential root uptake of a solute can be expressed by the following equation, here applied to P:

$$P_{uptake}(j) = \pi . \Delta z . L_{rv}(j) . D . \frac{\rho^2 - 1}{G(\rho(j), \nu(j))} . C_p$$

where P_{uptake} is the monthly potential root uptake per unit root surface area (kgP/m^2/month), Δz is soil depth considered (m), L_{rv} is the monthly root length density (m/m^3), D is the coefficient of P diffusion (m^2/month), C_P is the mean concentration of orthophosphate ions in the soil solution in Δz (kgP/m^3), $G(\rho,\nu)$ is a dimensionless geometric function of a ratio of soil cylinder to root radius (ρ, dimensionless) and a uptake of water (ν, dimensionless). C_p was derived from inorganic labile P provided by Ringeval et al. (2017). The inorganic labile P was winsorized to 0.01% to prevent outliers in the soil P distribution that bias the global average (see the distribution in Fig. S3). This results in the prescription of the value of 2 grid-cells for each simulation out of the 1000 replicates. Δz is equal to 0.3m as considered in Ringeval et al. (2017).

Following (Mollier et al., 2008), $G(\rho,\nu)$ is simplified in the case of P for which diffusion is the main process of transport in soil, and depends on ρ only:

$$G(\rho) = \frac{1}{2}\left(\frac{1-3\rho^2}{4} + \frac{\rho^4 \ln(\rho)}{\rho^2 - 1}\right)$$

with ρ the normalized radius (-) expressed as:

$$\rho = \frac{1}{R_0 \sqrt{\pi L_{rv}}}$$

with L_{rv} and thus ρ vary with month (see below).

D is the coefficient of P diffusion in soil (m²/month) and the values used in this study were computed in (Kvakić et al., 2018). Briefly, D is given by the 'constant slope impedance factor' model, that mimics the decrease in solute diffusivity from the P diffusivity in water (D_0) with lower soil water content. As the soil water content used in (Kvakić et al., 2018) corresponds to irrigated conditions, D is close to D_0, i.e. 2.277e^{-3} m²/month.

The monthly root length density (i.e. the length of root per volume of soil, m/m^3) is computed as follows:

$$L_{rv}(j)=\frac{C_{root}(j)*SRL}{\Delta z}$$

where C_{root} is the root biomass (in gDM/m^2), SRL is the specific root length (m/gDM). The following values were used for SRL: 74 (wheat), 100 (maize) and 146 m/gDM (rice) as used in Kvakić et al. (2018).

C_{root} is computed as follows:

$$C_{root}(j)=\frac{C_{root;LPJmL}(j)}{C_{root;LPJmL;max}}.\frac{RSR}{HI}.Y_{pot} \qquad \text{(Eq.S25)}$$

where Y_{pot} is the potential yield provided by Mueller et al. (2012) (expressed here in gDM/m^2 for the year considered), $C_{root;LPJmL}$ is the average monthly root biomass simulated by LPJmL (gDM/m²) and $C_{root;LPJmL;max}$ is the yearly maximum of $C_{root;LPJmL}$ (gDM/m²). HI and RSR are the harvest index and root/shoot ratio (dimensionless) and are described in Table S1. The ratio $\frac{C_{root;LPJmL}(m)}{C_{root;LPJmL;max}}$ varies between 0 and 1 and allows the introduction of seasonality in root biomass.

LPJmL (von Bloh et al., 2018) is one the Global Gridded Crop Models (GGCM) participating in a recent intercomparison (Elliott et al., 2015). Because of the divergence in simulated potential yields between GGCMs and the mismatch between the GGCMs and potential yield given by Mueller et al. (2012) (used in particular in our approach to compute the nutrient demand) (not shown), we chose to keep only the seasonality simulated by one GGCM instead ofusing the simulated root biomass directly. This allows consistency between computation of nutrient (N and P) demands and the P supply. The LPJmL simulation used to provide $C_{root;LPJmL}$ and $C_{root;LPJmL;max}$ in the above equation was performed by assuming the absence of nutrient limitation (called "harm-suffN" in Müller et al. (2017) and "harmnon" in Elliott et al. (2015)) and irrigated conditions following the protocol of the GGCM intercomparison. LPJmL considered spring and winter wheat and here we used the most productive one if both were simulated in the same grid-cell.

Text S4. Computation of N in residues remaining on cropland soil (N_{res})

N in residues remaining on cropland soil is called N_{res} in the Main Text. Here, to be consistent with the equations used for P in the Supp.Inf of Ringeval et al. (2017), we called it $R_{not\text{-}rm}$ (for residue not removed from cropland soil) :
for any grid-cell g, $N_{res}(g)=R_{not-rm}(g)$.

$R_{not\text{-}rm}$ was computed from N in harvest (H) provided by Bouwman et al. (2011) and few parameters constant at the global scale, as follows :

$$R_{not-rm}(g)=(r_{U/H}-1).r_R.H(g) \qquad (1)$$

with g : the grid-cell, $r_{U/H}$ is the ratio between uptake and harvest and r_R is the ratio between residues remaining on the cropland soil and total residues.

How to get (1) ?

For any grid-cell g, we have the following equations :

$$U(g)=H(g)+R_{tot}(g)$$

$$R_{tot}(g)=R_{not-rm}(g)+R_{rm}(g)$$

where U: uptake; H: harvest; R_{tot}: total residue; R_{rm}: residue removed from field; $R_{not\text{-}rm}$: biomass remaining on/within the soil after harvesting. All variables are N fluxes. The variable $R_{not\text{-}rm}$ includes root biomass if the harvest is aboveground.

These equations are also correct at the global scale, i.e.

$$\overline{U}=\overline{H}+\overline{R_{tot}} \qquad (2)$$

$$\overline{R_{tot}}=\overline{R_{not-rm}}+\overline{R_{rm}} \qquad (3)$$

where overlined variables are variables computed at the global scale.

We defined the following parameters at the global scale:

$$r_{U/H}=\overline{U}/\overline{H} \qquad (4)$$

$$r_R=\overline{R_{not-rm}}/\overline{R_{tot}} \qquad (5)$$

The values of such parameters, considered as constant in space, were computed thanks to (Smil, 2000) (see next paragraph).

By injecting the definition of r_R in (2) and then rearranging, we get: $\overline{R_{not-rm}}=(\overline{U}-\overline{H}).r_R$.
Then, by injecting the definition of $r_{U/H}$, we obtained: $\overline{R_{not-rm}}=(r_{U/H}-1).r_R.\overline{H}$.

We applied this equation for any grid-cell, i.e. :

$$R_{not-rm}(g)=(r_{U/H}-1).r_R.H(g)$$

(Bouwman et al., 2011) provide harvest for cropland (H) for any grid-cell and we use two parameters defined at the global scale to derive $R_{not\text{-}rm}$ from H for each grid-cell.

Global values used for $r_{U/H}$ and r_R

By definition, we have :

$$r_{U/H}=\overline{U}/\overline{H} \qquad (4)$$

$$r_R=\overline{R_{not-rm}}/\overline{R_{tot}} \qquad (5)$$

For some crop categories, (Smil, 1999) provided the following variables at the global scale : harvest ($\overline{H}$), total shoot residue ($\overline{R_{tot}^{shoot}}$) and shoot N uptake ($\overline{U^{shoot}}$) (Table 2 of (Smil, 1999)). Values of $\overline{U^{shoot}}$, $\overline{H}$ and $\overline{R_{tot}^{shoot}}$ corresponding to global cropland are estimated by computing a sum of the different crop categories (excluding forage) ; and $\overline{H}$, $\overline{R_{tot}^{shoot}}$ and $\overline{U^{shoot}}$ are equal to 50, 25 and 75 TgN/yr, respectively. In the following, we expressed $r_{U/H}$ and r_R with $\overline{H}$, $\overline{R_{tot}^{shoot}}$ and $\overline{U^{shoot}}$.

Global cropland U can be decomposed within the uptake for shoot biomass and the uptake for root biomass, i.e. : $\overline{U}=\overline{U^{shoot}}+\overline{U^{root}}$. Thus, $\overline{U}=\overline{U^{shoot}}.(1+RSR_N)$ with RSR_N the ratio between N in root and N in shoot. We get :

$$r_{U/H}=\overline{U^{shoot}}.(1+RSR_N)/\overline{H} \qquad (6).$$

By combining parameters definition given in Table S1, we can express RSR_N as follows :

$$RSR_N=\frac{NHI}{HI}.\frac{N_{\%,root}}{N_{\%,grain}}.RSR$$

By using parameters values given in Table S1 for maize, we found RSR_N equal to 0.16. Finally, we found a $r_{U/H}$ equal to 1.74.

By decomposing (5) into roots and shoots, we get :

$$r_R=\frac{\overline{R_{not-rm}^{shoot}+R_{not-rm}^{root}}}{\overline{R_{tot}^{shoot}}+\overline{R_{tot}^{root}}} \qquad (7).$$

We assume that all root biomass remains within the soil as residue (which is wrong for « root, tubers » but true for other crops categories considered in (Smil, 1999)), i.e. $\overline{R_{not-rm}^{root}}=\overline{R_{tot}^{root}}$ (no residue concerning root is removed), $\overline{H^{root}}=0$ (harvest concerns aboveground, not root) and thus, $\overline{R_{tot}^{root}}=\overline{U^{root}}$. Eq.7 can be re-written as follows :

$$r_R=\frac{\overline{R_{not-rm}^{shoot}}+\overline{U^{root}}}{\overline{R_{tot}^{shoot}}+\overline{U^{root}}} \quad .$$

(Smil, 2000) approached aboveground crop residue removed from the field by half of the total aboveground residue, thus: $r_R=\frac{0.5*\overline{R_{tot}^{shoot}}+\overline{U^{root}}}{\overline{R_{tot}^{shoot}}+\overline{U^{root}}}$. Finally, by using RSR_N as described above, we find:

$$r_R=\frac{0.5*\overline{R_{tot}^{shoot}}+RSR_N.\overline{U^{shoot}}}{\overline{R_{tot}^{shoot}}+RSR_N.\overline{U^{shoot}}} \qquad (8).$$

We found a r_R equal to 0.7.

Text S5. Spatial distribution of R_N, R_P, R_{NP}

At the global scale, the limitation by N is larger than that by P, when N and P are considered as independent, especially for maize (R_N=0.52±0.00; R_P=0.61±0.01) and wheat (R_N=0.60±0.00; R_P=0.72±0.00) (Table 3 of the Main Text). The spatial distributions of R_N and R_P are very different (Fig. S4 for maize), leading to all combinations possible (high N and P limitations, high N limitation and low P limitation, etc.) (Fig. S5). Taking maize as an example, we found that: India and China are not severely limited by any of the nutrients (e.g. for China: R_N=0.69; R_P=0.78), the USA is moderately limited in both nutrients (R_N=0.54; R_P=0.47), Western Europe is more N- than P-limited (e.g. for Spain: R_N=0.31; R_P=0.96) and, the Western Russian Federation and Ukraine are severely limited in both N and P (e.g. for Ukraine: R_N=0.18; R_P=0.13) (Fig. S5).

When N and P are considered in interaction, we found that nutrient limitation is common with the exception of China, India and to a lesser extent, Western Europe and Eastern USA (Fig. S5). Consequently, the global supply/demand ratio R_{NP} drops to ~0.35 (Table 3). Our study indicates that the interaction is a process that must be considered in the estimates of nutrient limitation. In our approach, regions with low NP limitations are restricted to China, India and to a lesser extent, Western Europe and Eastern USA. Some elements support these findings. Previous studies partly based on substance flow analysis show very positive current soil nutrient balances in China (Liu et al., 2010; Ma et al., 2010). Croplands of China, India, and the USA together account for ~65% of global N and P excess (West et al., 2014). We found that Western Europe is more N-limited than P-limited. Despite a decrease in soil P input following improvements in fertilization reasoning since 1970 in Western European countries (Senthilkumar et al., 2012), P accumulated in soils during the past decades can still be used by plants (Ringeval et al., 2014). This legacy effect does not exist for N, and N fertilisation rates are now increasingly limited by environmental regulations in many Western European countries (European Commission, 2018). N stress was found to occur in Spain and France in a study performed with EPIC (Fig. 7 of Balkovič et al. (2013)) and in Schils et al. (2018). We found that the USA is moderately limited in both nutrients with contrasting behaviour between the centre of the USA (low R_{NP}) and the East (high R_{NP}). Spatial heterogeneity has been underlined at the Mississippi watershed scale by Jacobson et al. (2011) where there are large inputs of P fertilizers in the Corn Belt. Some modeling difficulties related to the representation of soil P dynamics in our approach could also contribute to an overestimation of P limitation in the USA. Soils in the center of the USA are in particular represented by Mollisols, which are characterized by high content of soil organic carbon and substantial carbonate content, both with opposite effect on the P in soil solution (Achat et al., 2016). Carbonate could decrease P concentration of soil P solution thanks to reaction of precipitation (Tunesi et al., 1999). While our approach takes into account P exchange between the soil solution and inorganic labile P (either P fixed on soil particles or P involved in precipitates), it does so by considering the long-term equilibrium. This may be not relevant for the representation of fertilizer application onto soils that precipitate phosphate (e.g. with carbonate). The same reasoning should apply for high-fixing capacity soils (e.g. oxisols whose oxides of aluminium and iron lead to high adsorption of P ions onto soil particles).

A recent meta-analysis compiled P-fertilization experiments (Hou et al., 2020). Contrary to previous meta-analysis dealing with fertilization experiments (e.g Augusto et al.

(2017); Elser et al. (2007); Li et al. (2016); Yue et al. (2016)), Hou et al. (2020) distinguish cropland to other ecosystems. However, they treat only P and do not consider N or NxP interaction. Some results found by Hou et al. (2020) are consistent to results found here (large limitation by P at the global scale, some tropical areas not limited by P, part of US limited by P) while some mismatch exists (e.g. some sites in China are P-limited in (Hou et al., 2020) vs China and India are not nutrient-limited in our study). Besides, as mentioned in the main Text of our study, Hou et al. (2020) underlines the difficulty to use fertilization experiment in croplands (no record of history of fertilization, etc.). (Yue et al., 2016) also included croplands in their meta-analysis. However, they did not particularly focus on NxP interactions, but on many factors (CO_2, temperature, water). In practice, the croplands that were studied in this meta-analysis are almost all only N-fertilised.

Text S6. Relationship between R_{NP} and yield gap

The relationship between the yield gap (Y_{real}/Y_{pot}, with Y_{real} and Y_{pot} being the actual and potential yield, respectively) and R_{NP} was assessed. This was done at country scale. Actual yield (Y_{real}) could diverge to potential yield (Y_{pot}) due to many factors: limiting nutrients (N, P but also potassium, etc.), limiting water and pest/diseases. Nutrient limitation when both N and P are considered (R_{NP}) is supposed to be closer to the actual nutrient limitation than the one considering only one nutrient (either N or P). That is why we restrict our analysis to the relationship between nutrient limitation and yield gap to R_{NP}. Y_{real}/Y_{pot} was provided by Mueller et al. (2012). The Y_{real}/Y_{pot} ratio is used as a measure of the yield gap and is a function of nutrient limitations, water limitation, pest and diseases, etc. Please, note nevertheless that the potential yield is both used in the yield gap and here-computed R_{NP}. Country values of R_{NP} and Y_{real}/Y_{pot} were computed by considering only grid-cells for which our analysis provides R_{NP} values (Table S2) and by using crop-area (Ramankutty et al., 2008) as weight. A negative exponential model g ($g: x \rightarrow 1-\beta.\exp(-x)$, with β the constant calibrated) was fit using ordinary least squares. The portion of variance in Y_{real}/Y_{pot} explained by R_{NP} was estimated with the coefficient of determination (R^2). We investigated how a third variable could modulate the relationship between the yield and R_{NP}. To do this, we divided all countries into 4 equal quarters based on the quartiles of this third variable ([minimum, $Q1$[, [$Q1$, $Q2$[, [$Q2$, $Q3$[and [$Q3$, maximum], where $Q1$, $Q2$, $Q3$ are the quartiles of the third variable) and computed R^2 of g for each quarter. We checked that the change in R^2 found when focusing on quarters is not explained by a reduction in the numbers of countries considered by using random country subsets. The variables chosen as the third variable are related to other limiting factors (irrigated fraction for the crop considered, or precipitation or pesticide use per agricultural area). The analysis was restricted to the country scale because most of these variables are available at that scale only. Irrigated fractions for each crop are given by MIRCA (Portmann et al., 2010), precipitation is provided by CRU (Mitchell & Jones, 2005) and pesticide use (and agricultural area used to compute the pesticide use per ha) is derived from FAOSTAT (Food and Agriculture Organization of the United Nations (FAO) Statistical database (FAOSTAT), n.d.). All variables are representative of the year 2000.

At country-scale, the spatial variance of Y_{real}/Y_{pot} explained by a negative exponential fit against R_{NP} (measured with R^2) is small: 0.12 for maize (Fig. S7), 0.08 for wheat (not shown) and 0.26 for rice (not shown), a crop that is usually grown with sufficient irrigation. A small R^2 could be explained by other factors limiting yield (e.g. insufficient water) whose spatial distribution might be different to that of R_{NP}. For maize, we found that overall, R^2 increases when it is computed on subsets of countries characterized by more homogeneous water conditions, approached here by the national crop area fraction irrigated (Fig. S7, panels b-e) or the amount of precipitation (Fig. S7, panels h-k). Quarters with smallest fractions of irrigated maize (Fig. S7 b-c) or with largest precipitation (Fig. S7 i-k) have a R^2 larger than the R^2 computed for all countries (Fig. S7, first column). The increase in R^2 when sampling countries with homogeneous irrigation practices or precipitation is found for wheat (not shown), but not for rice (not shown). We did not find any increase in R^2 when countries are segregated according to the amount of pesticides used per agricultural area (third row of Fig. S7 for maize). The weight of individual country on the R^2 values has been assessed through an influence plot and Cook's distances, which do not show any unreasonable influence of a given country (not shown).

References

Achat, D. L., Pousse, N., Nicolas, M., Brédoire, F., & Augusto, L. (2016). Soil properties controlling inorganic phosphorus availability: general results from a national forest network and a global compilation of the literature. *Biogeochemistry*, *127*(2–3), 255–272. https://doi.org/10.1007/s10533-015-0178-0

Amos, B., & Walters, D. T. (2006). Maize Root Biomass and Net Rhizodeposited Carbon. *Soil Science Society of America Journal*, *70*(5), 1489. https://doi.org/10.2136/sssaj2005.0216

Augusto, L., Achat, D. L., Jonard, M., Vidal, D., & Ringeval, B. (2017). Soil parent material-A major driver of plant nutrient limitations in terrestrial ecosystems. *Global Change Biology*. https://doi.org/10.1111/gcb.13691

Balkovič, J., van der Velde, M., Schmid, E., Skalský, R., Khabarov, N., Obersteiner, M., et al. (2013). Pan-European crop modelling with EPIC: Implementation, up-scaling and regional crop yield validation. *Agricultural Systems*, *120*, 61–75. https://doi.org/10.1016/j.agsy.2013.05.008

Bouwman, L., Goldewijk, K. K., Van Der Hoek, K. W., Beusen, A. H. W., Van Vuuren, D. P., Willems, J., et al. (2011). Exploring global changes in nitrogen and phosphorus cycles in agriculture induced by livestock production over the 1900-2050 period. *Proceedings of the National Academy of Sciences*. https://doi.org/10.1073/pnas.1012878108

Elliott, J., Müller, C., Deryng, D., Chryssanthacopoulos, J., Boote, K. J., Büchner, M., et al. (2015). The Global Gridded Crop Model Intercomparison: data and modeling protocols for Phase 1 (v1.0). *Geoscientific Model Development*, *8*(2), 261–277. https://doi.org/10.5194/gmd-8-261-2015

Elser, J. J., Bracken, M. E. S., Cleland, E. E., Gruner, D. S., Harpole, W. S., Hillebrand, H., et al. (2007). Global analysis of nitrogen and phosphorus limitation of primary producers in freshwater, marine and terrestrial ecosystems. *Ecology Letters*, *10*(12), 1135–1142. https://doi.org/10.1111/j.1461-0248.2007.01113.x

European Commission. (2018, April 5). Report on the implementation of Council Directive 91/676/EEC concerning the protection of waters against pollution caused by nitrates from agricultural sources based on Member State reports for the period 2012–2015 (

http://ec.europa.eu/environment/water/water-nitrates/pdf/nitrates_directive_implementation_report.pdf).

Food and Agriculture Organization of the United Nations (FAO) Statistical database (FAOSTAT). (n.d.). Retrieved from http://faostat3.fao.org/faostat-gateway/go/to/home/E

Górny, A. G., & Garczyński, S. (2008). Nitrogen and Phosphorus Efficiency in Wild and Cultivated Species of Wheat. *Journal of Plant Nutrition*, *31*(2), 263–279. https://doi.org/10.1080/01904160701853878

Harpole, W. S., Ngai, J. T., Cleland, E. E., Seabloom, E. W., Borer, E. T., Bracken, M. E. S., et al. (2011). Nutrient co-limitation of primary producer communities: Community co-limitation. *Ecology Letters*, *14*(9), 852–862. https://doi.org/10.1111/j.1461-0248.2011.01651.x

Hergoualc'h, K. (2019). Chapter 11: N 2 O Emissions from Managed Soils, and CO 2 Emissions from Lime and Urea Application. In *2019 Refinement to the 2006 IPCC Guidelines for National Greenhouse Gas Inventories*. Retrieved from https://www.ipcc-nggip.iges.or.jp/public/2019rf/pdf/4_Volume4/19R_V4_Ch11_Soils_N2O_CO2.pdf

Hocking, P. J. (1994). Dry-matter production, mineral nutrient concentrations, and nutrient distribution and redistribution in irrigated spring wheat. *Journal of Plant Nutrition*, *17*(8), 1289–1308. https://doi.org/10.1080/01904169409364807

Hou, E., Luo, Y., Kuang, Y., Chen, C., Lu, X., Jiang, L., et al. (2020). Global meta-analysis shows pervasive phosphorus limitation of aboveground plant production in natural terrestrial ecosystems. *Nature Communications*, *11*(1), 637. https://doi.org/10.1038/s41467-020-14492-w

Hütsch, B. W., & Schubert, S. (2017). Harvest Index of Maize (Zea mays L.): Are There Possibilities for Improvement? In *Advances in Agronomy* (Vol. 146, pp. 37–82). Elsevier. https://doi.org/10.1016/bs.agron.2017.07.004

Jacobson, L. M., David, M. B., & Drinkwater, L. E. (2011). A Spatial Analysis of Phosphorus in the Mississippi River Basin. *Journal of Environment Quality*, *40*(3), 931. https://doi.org/10.2134/jeq2010.0386

Kvakić, M., Pellerin, S., Ciais, P., Achat, D. L., Augusto, L., Denoroy, P., et al. (2018). Quantifying the Limitation to World Cereal Production Due To Soil Phosphorus Status. *Global Biogeochemical Cycles*. https://doi.org/10.1002/2017GB005754

Latshaw, W. L., & Miller, E. C. (1924). Elemental composition of the corn plant. *Journal of Agricultural Research*, *27*(11), 845–61.

Li, W., Ciais, P., Wang, Y., Peng, S., Broquet, G., Ballantyne, A. P., et al. (2016). Reducing uncertainties in decadal variability of the global carbon budget with multiple datasets. *Proceedings of the National Academy of Sciences*, *113*(46), 13104–13108. https://doi.org/10.1073/pnas.1603956113

Liu, J., You, L., Amini, M., Obersteiner, M., Herrero, M., Zehnder, A. J. B., & Yang, H. (2010). A high-resolution assessment on global nitrogen flows in cropland. *Proceedings of the National Academy of Sciences*, *107*(17), 8035–8040. https://doi.org/10.1073/pnas.0913658107

Ma, L., Ma, W. Q., Velthof, G. L., Wang, F. H., Qin, W., Zhang, F. S., & Oenema, O. (2010). Modeling Nutrient Flows in the Food Chain of China. *Journal of Environment Quality*, *39*(4), 1279. https://doi.org/10.2134/jeq2009.0403

Mitchell, T. D., & Jones, P. D. (2005). An improved method of constructing a database of monthly climate observations and associated high-resolution grids. *International Journal of Climatology*, *25*(6), 693–712. https://doi.org/10.1002/joc.1181

Mollier, A., De Willigen, P., Heinen, M., Morel, C., Schneider, A., & Pellerin, S. (2008). A two-dimensional simulation model of phosphorus uptake including crop growth and P-response. *Ecological Modelling*, *210*(4), 453–464. https://doi.org/10.1016/j.ecolmodel.2007.08.008

Mueller, N. D., Gerber, J. S., Johnston, M., Ray, D. K., Ramankutty, N., & Foley, J. A. (2012). Closing yield gaps through nutrient and water management. *Nature*, *490*(7419), 254–257. https://doi.org/10.1038/nature11420

Müller, C., Elliott, J., Chryssanthacopoulos, J., Arneth, A., Balkovic, J., Ciais, P., et al. (2017). Global gridded crop model evaluation: benchmarking, skills, deficiencies and implications. *Geoscientific Model Development*, *10*(4), 1403–1422. https://doi.org/10.5194/gmd-10-1403-2017

Portmann, F. T., Siebert, S., & Döll, P. (2010). MIRCA2000-Global monthly irrigated and rainfed crop areas around the year 2000: A new high-resolution data set for agricultural and hydrological modeling: MONTHLY IRRIGATED AND RAINFED CROP AREAS. *Global Biogeochemical Cycles*, *24*(1), n/a-n/a. https://doi.org/10.1029/2008GB003435

Ramankutty, N., Evan, A. T., Monfreda, C., & Foley, J. A. (2008). Farming the planet: 1. Geographic distribution of global agricultural lands in the year 2000. *Global Biogeochemical Cycles*, *22*(1), n/a-n/a. https://doi.org/10.1029/2007GB002952

Ringeval, B., Nowak, B., Nesme, T., Delmas, M., & Pellerin, S. (2014). Contribution of anthropogenic phosphorus to agricultural soil fertility and food production. *Global Biogeochemical Cycles*, *28*(7), 743–756. https://doi.org/10.1002/2014GB004842

Ringeval, Bruno, Augusto, L., Monod, H., van Apeldoorn, D., Bouwman, L., Yang, X., et al. (2017). Phosphorus in agricultural soils: drivers of its distribution at the global scale. *Global Change Biology*. https://doi.org/10.1111/gcb.13618

Rose, T. J., Pariasca-Tanaka, J., Rose, M. T., Fukuta, Y., & Wissuwa, M. (2010). Genotypic variation in grain phosphorus concentration, and opportunities to improve P-use efficiency in rice. *Field Crops Research*, *119*(1), 154–160. https://doi.org/10.1016/j.fcr.2010.07.004

Schils, R., Olesen, J. E., Kersebaum, K.-C., Rijk, B., Oberforster, M., Kalyada, V., et al. (2018). Cereal yield gaps across Europe. *European Journal of Agronomy*, *101*, 109–120.

Senthilkumar, K., Nesme, T., Mollier, A., & Pellerin, S. (2012). Conceptual design and quantification of phosphorus flows and balances at the country scale: The case of France. *Global Biogeochemical Cycles*, *26*(GB2008), GB2008. https://doi.org/10.1029/2011GB004102

Smil, V. (1999). Nitrogen in crop production: an account of global flows. *Global Biogeochemical Cycles*, *13*(2), 647–662. https://doi.org/0886-6236/99/1999GB900015512.00

Smil, V. (2000). Phosphorus in the environment: natural flows and human interferences. *Annual Review of Energy and the Environment*, *25*(1), 53–88.

Tunesi, S., Poggi, V., & Gessa, C. (1999). Phosphate adsorption and precipitation in calcareous soils: the role of calcium ions in solution and carbonate minerals. *Nutrient Cycling in Agroecosystems*, *53*, 219–227.

Van Duivenbooden, N. (1992). *Sustainability in terms of nutrient elements with special reference to*

West-Africa. CABO-DLO.

von Bloh, W., Schaphoff, S., Müller, C., Rolinski, S., Waha, K., & Zaehle, S. (2018). Implementing the nitrogen cycle into the dynamic global vegetation, hydrology, and crop growth model LPJmL (version 5.0). *Geoscientific Model Development, 11*(7), 2789–2812. https://doi.org/10.5194/gmd-11-2789-2018

West, P. C., Gerber, J. S., Engstrom, P. M., Mueller, N. D., Brauman, K. A., Carlson, K. M., et al. (2014). Leverage points for improving global food security and the environment. *Science, 345*(6194), 325–328.

Williams, J. D., McCool, D. K., Reardon, C. L., Douglas, C. L., Albrecht, S. L., & Rickman, R. W. (2013). Root: shoot ratios and belowground biomass distribution for Pacific Northwest dryland crops. *Journal of Soil and Water Conservation, 68*(5), 349–360.

WILLIGEN, P. D., & NOORDWIJK, M. V. (1994). MASS FLOW AND DIFFUSION OF NUTRIENTS TO A ROOT WITH CONSTANT OR ZERO-SINK UPTAKE II. ZERO-SINK UPTAKE. *Soil Science,* pp. 171–175.

Wissuwa, M., & Ae, N. (2001). Genotypic variation for tolerance to phosphorus deficiency in rice and the potential for its exploitation in rice improvement. *Plant Breeding, 120*(1), 43–48.

Ye, Y., Liang, X., Chen, Y., Li, L., Ji, Y., & Zhu, C. (2014). Carbon, Nitrogen and Phosphorus Accumulation and Partitioning, and C:N:P Stoichiometry in Late-Season Rice under Different Water and Nitrogen Managements. *PLoS ONE, 9*(7), e101776. https://doi.org/10.1371/journal.pone.0101776

Yue, K., Fornara, D. A., Yang, W., Peng, Y., Li, Z., Wu, F., & Peng, C. (2016). Effects of three global change drivers on terrestrial C:N:P stoichiometry: a global synthesis. *Global Change Biology*. https://doi.org/10.1111/gcb.13569

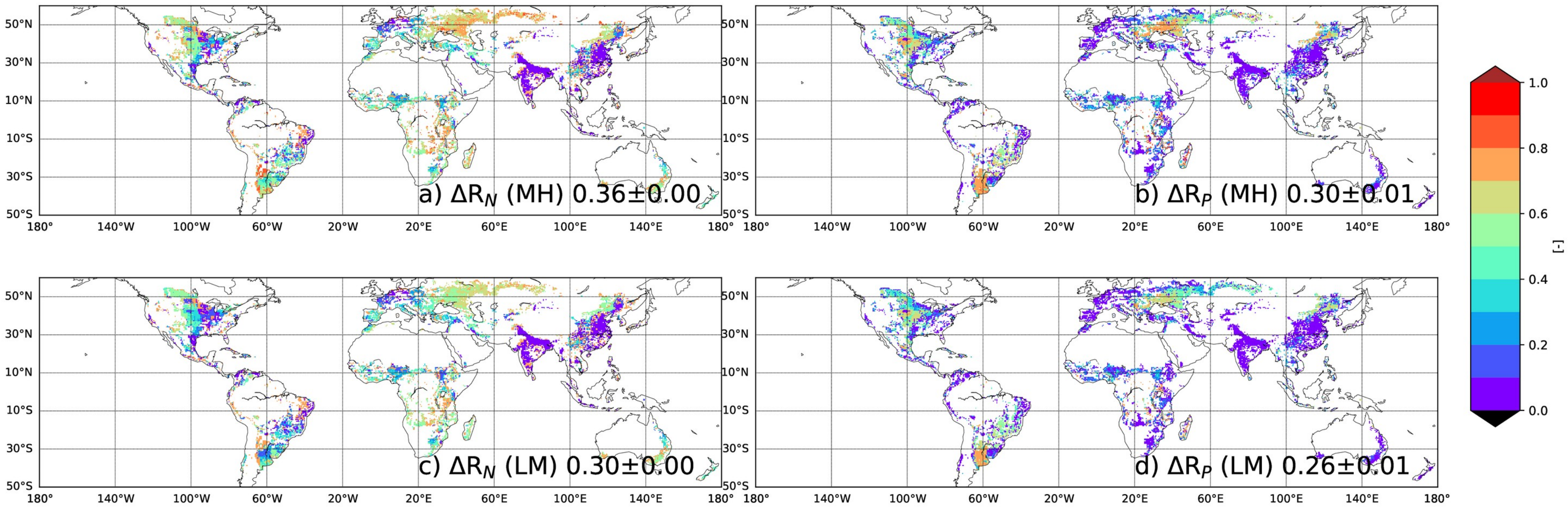

Figure S1. For maize, the spatial distribution of increase in R_N (left) and R_P (right) required at the same time to make R_{NP} equal to 0.75. The increases are computed with MH (top) and LM (bottom) formalisms. Global averaged values and one standard-deviation are provided in the right bottom corner of each panel.

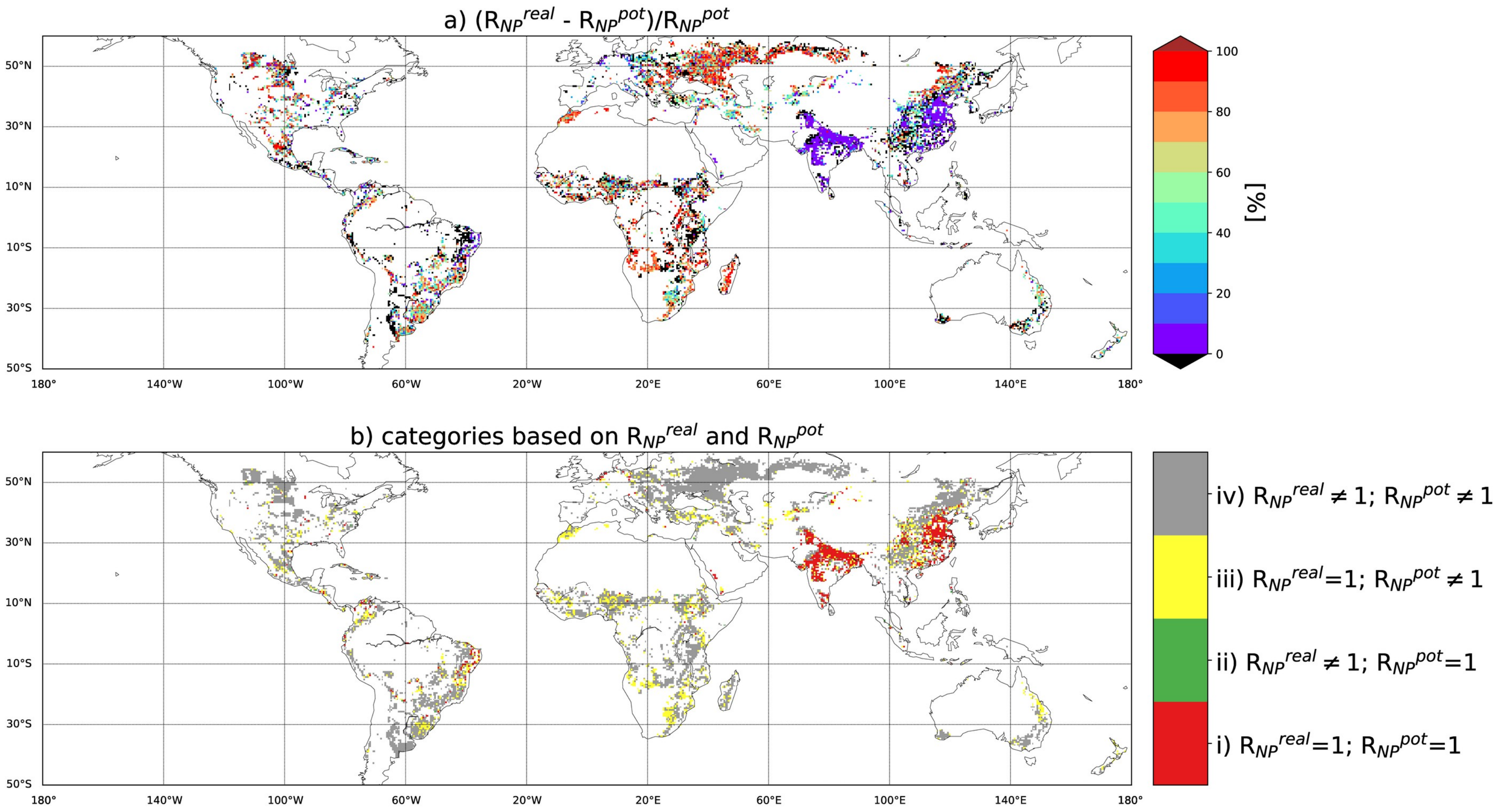
a) $(R_{NP}^{real} - R_{NP}^{pot})/R_{NP}^{pot}$

b) categories based on R_{NP}^{real} and R_{NP}^{pot}

Figure S2. The effect of using the acual yield (instead of potential yield) on the computed nutrient limitation. In the Main Text, the potential yield (Y_{pot}) is used to compute R_{NP} (through Eq.12 for the N and P demands and in a lesser extent in the P supply through Eq.S25 in Text S3). In this figure, we compared the NP limitation (R_{NP}) when computed with potential yield (called here R_{NP}^{pot}) as in the Main Text and the NP limitation when computed with Y_{real} (called here R_{NP}^{real}). Both Y_{pot} and Y_{real} are provided by Mueller et al. (2012). The figure shows the difference between R_{NP}^{pot} and R_{NP}^{real} (expressed in percentage of R_{NP}^{pot}, top) and some categories based on the values of R_{NP}^{pot} and R_{NP}^{real} (bottom). Only grid-cells with $Y_{real}<0.75*Y_{pot}$ are plotted in the two panels. The different categories used in the bottom panel can be interpreted as follows:

- Class i: $R_{NP}^{real}=1$ and $R_{NP}^{pot}=1$. The actual yield is not limited by NP but by other factors (because Y_{real} is smaller than Y_{pot}). Current NP supply would be sufficient to satisfy the demand if the limitation by these other factors was removed.
- Class ii: $R_{NP}^{real}\neq1$ and $R_{NP}^{pot}=1$. No grid-cell in this category. This is partly explained by the fact that R_{NP}^{real} is mostly greater than R_{NP}^{pot}.
- Class iii: $R_{NP}^{real}=1$ and $R_{NP}^{pot}\neq1$. The actual yield is not limited by NP but by other factors (because Y_{real} is smaller than Y_{pot}). Current NP supply would be insufficient to satisfy the demand if the limitation by these other factors was removed.
- Class iv: $R_{NP}^{real}\neq1$ and $R_{NP}^{pot}\neq1$. The actual yield is limited by NP and potentially by other factors.

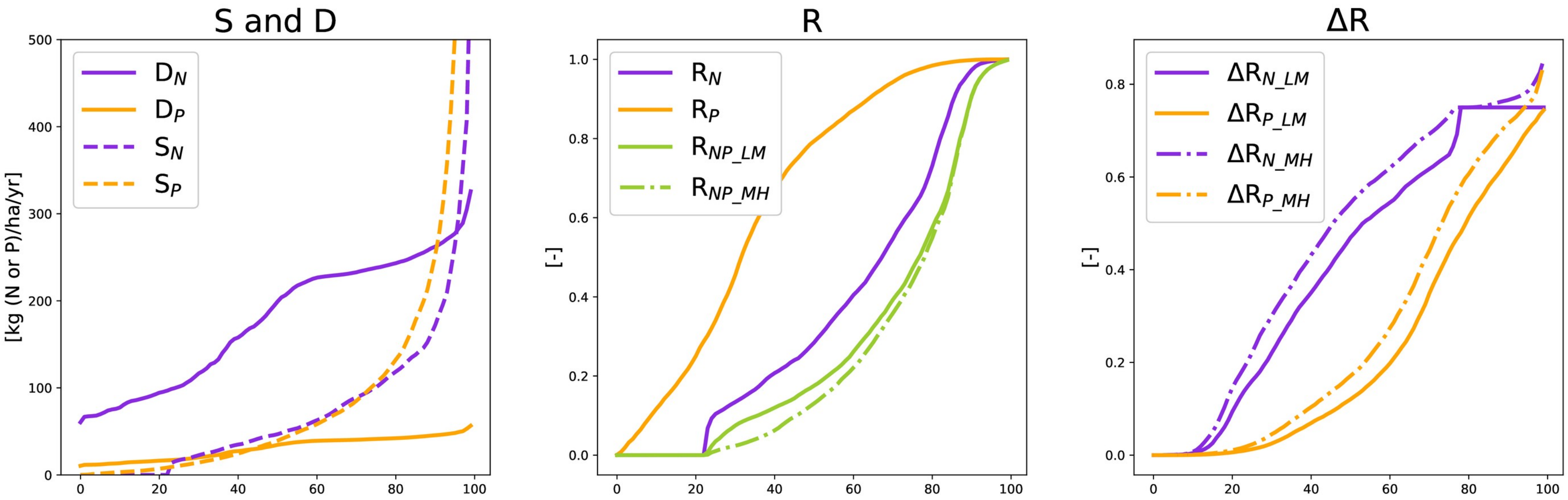

Figure S3. Grid-cell distribution in percentiles of different variables (*S*: supply, *D*: demand, *R*: supply/demand ratio, ΔR: increase in *R* required to make R_{NP}=0.75) for maize. Values plotted in this figure are not weighted by the cropland area of each grid-cell. 11565 grid-cells have been considered for maize in our approach (Table S2).

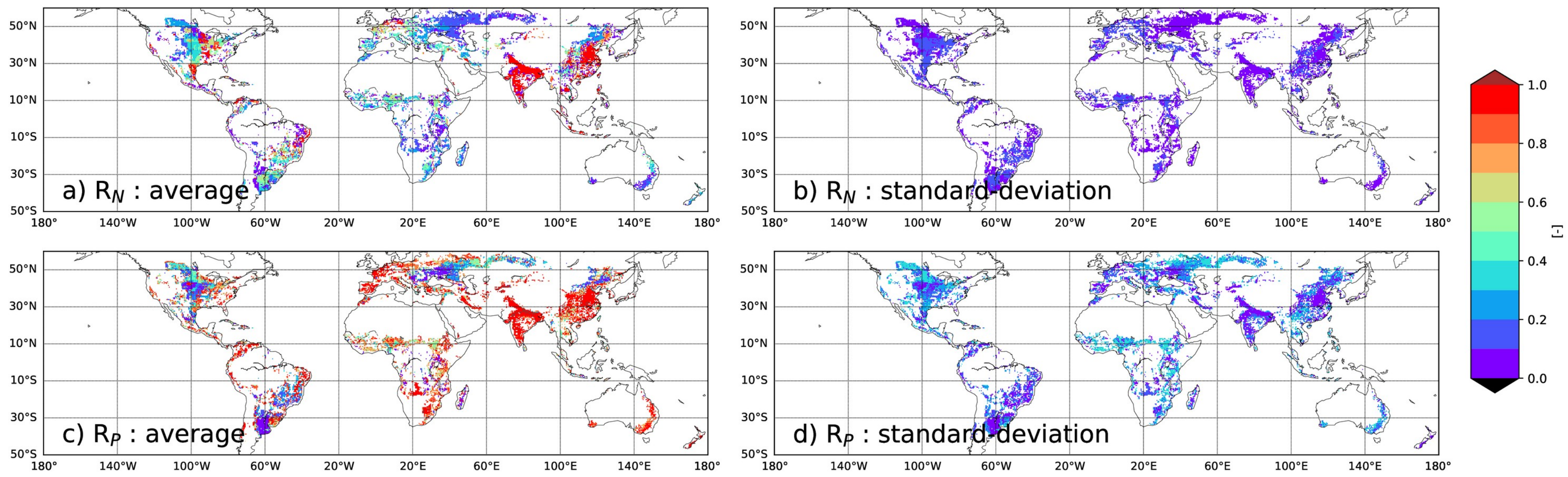

Figure S4. For maize, spatial distribution of R_N and R_P when N and P are considered as independent: average and standard-deviation of the 1000 replicates.

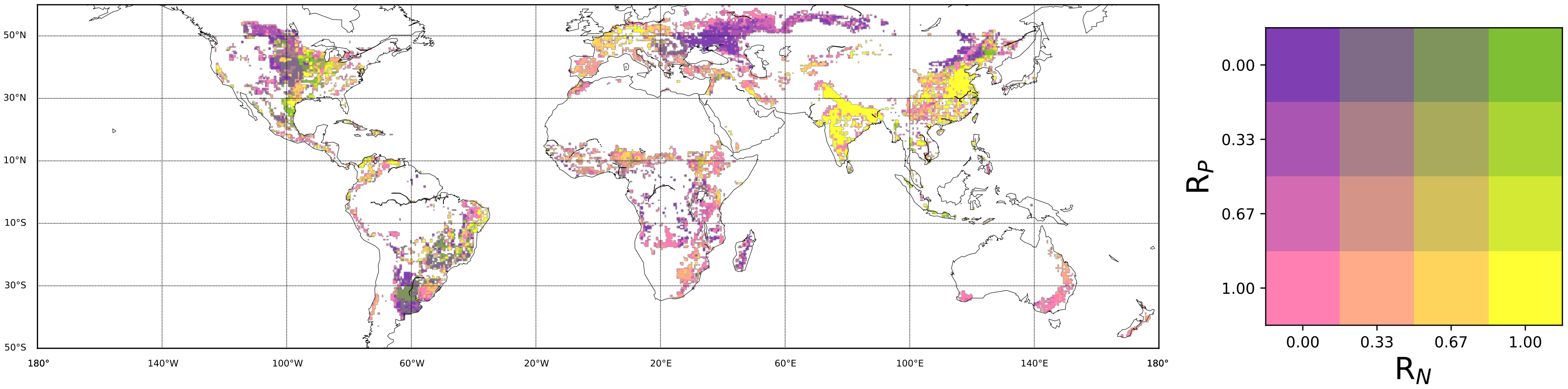

Figure S5. For maize, the spatial distribution of nutrient limitation when N and P are considered to be independent (bivariate plot of R_N and R_P).

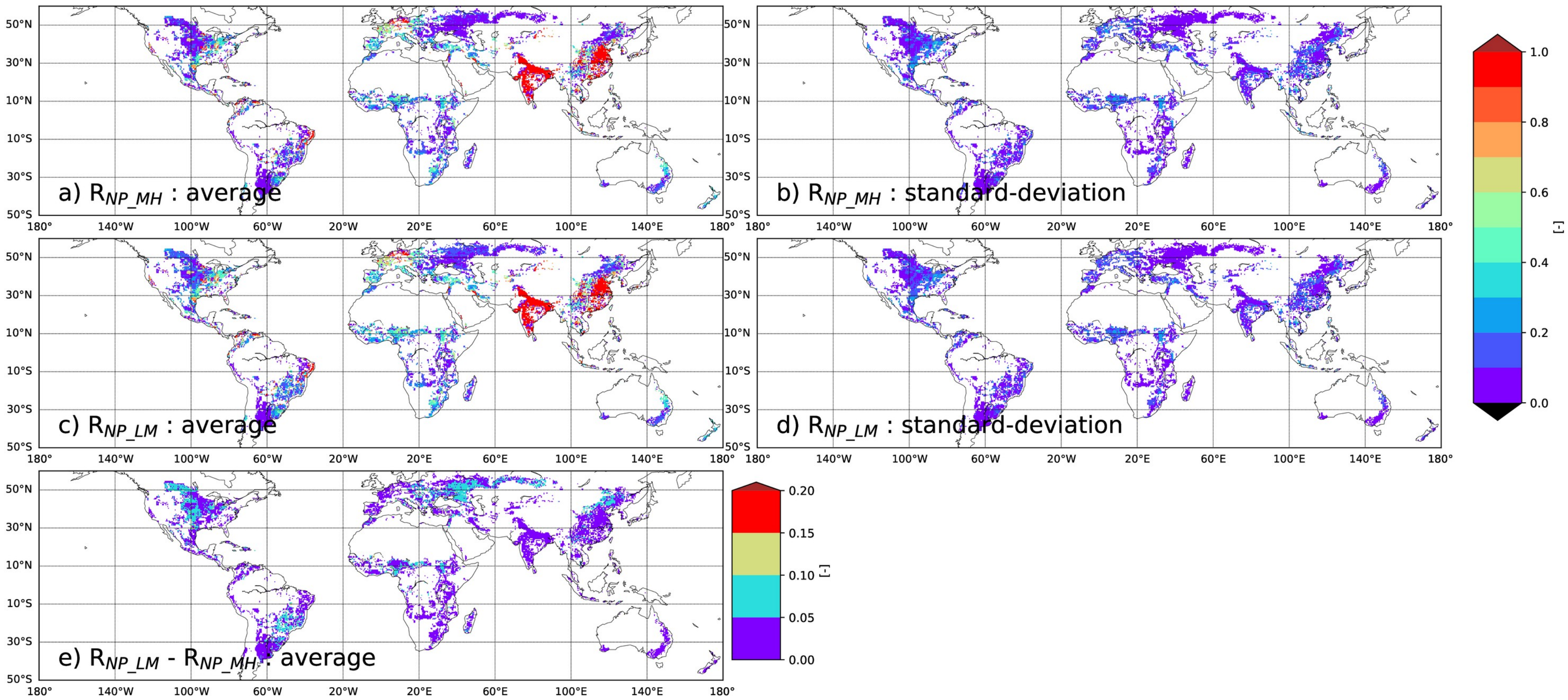

Figure S6. For maize, spatial distribution of R_{NP}: average and standard-deviation for both formalisms of interaction (a-b: MH; c-d: LM). The averaged difference of R_{NP} between LM and MH is also plotted (panel e).

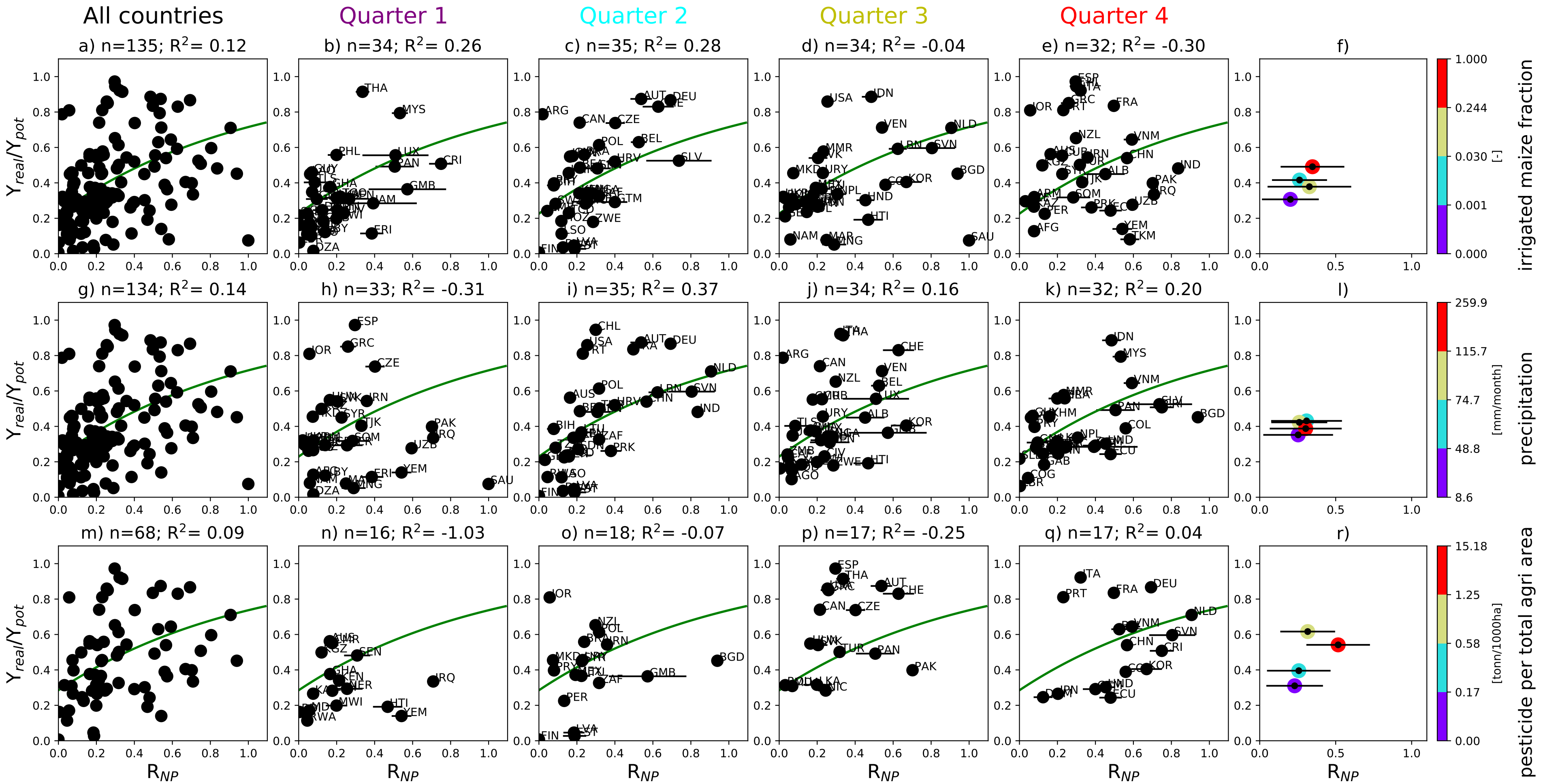

Figure S7. Scatterplots of the ratio Y_{real}/Y_{pot} provided by Mueller et al. (2012) vs. the simulated R_{NP} (here only computed by using the MH formalism for the purpose of simplicity) at the country scale for maize. Each dot corresponds to one country. In the extreme-left column, all countries are considered while columns 2-5 correspond to the different quarters based on the quartiles of a third variable (column 2: [minimum, Q1[, column 3: [Q1, Q2[, column 4: [Q2, Q3[, column 5: [Q3, maximum] with Q1-3 the quartiles of a third variable). The different rows correspond to different third variables used to distinguish the countries in quarters (top: irrigated fraction of maize, middle: precipitations, bottom: pesticide use per total agricultural area). The extreme-left panels vary among rows because we consider only countries for which data about the third variable is available. The green line corresponds to a negative exponential fit g ($g: x \rightarrow 1-\beta.exp(-x)$). The fit is made for each extreme-left panels (a, g, m) and reported in columns 2-5 of the same row. The number of countries considered (called n in the title of each panel), as well as the R^2 for the fit computed on all countries are given for each panel. The name of the country (ISO nomenclature) is given for each panel of columns 2-5. The extreme-right panels (l, f, r) provide the average of countries considered in each quarter and the boundaries of the colour palet are defined by (min, Q1, Q2, Q3, max). The error bars of panels b-e, h-k and n-q correspond to the standard-deviation arising from the 1000 simulations described in the Main Text. In panels f, l and r, the error bars correspond to the standard-deviation arising from the different countries within each quarter.

Table S1. Parameters used to estimate the N and P demands (D_N and D_P, respectively). Values in the Table are representative of plant maturity and were taken from field experiments (rather than hydroponic experiments) if possible (this is still not the case for roots).

Crop-specific values for N and P concentrations organs were derived from field experiments in stressed conditions focusing on the lower, linear part of the uptake-yield curve when nutrient use efficiency is maximal. Consequently, the nutrient demand estimates correspond to the minimum amount of nutrients required to achieve a certain grain yield. Mean values are shown with their standard error. If a standard error was not provided in the source material, a coefficient of variation of 20% was assumed. *DM* used in the column “Unit” refers to Dry Matter. X_{organ} with *X* in {*C, N, P*} and *organ* in {*root, shoot, grain*} are in gX. γ is a converting factor equal to 0.45e^{+3} gC/kgDM.

Variable	Unit	Name	Definition	Maize	Wheat	Rice
RSR	[-]	Root/shoot ratio	$\frac{C_{root}}{C_{shoot}}$	0.16 (Amos & Walters, 2006)	0.15 (Williams et al., 2013)	0.15 ± 0.07 (Wissuwa & Ae, 2001)
HI	[-]	Harvest index	$\frac{C_{grain}}{C_{shoot}}$	0.53 (Hütsch & Schubert, 2017)	0.51 (Hütsch & Schubert, 2017)	0.51 ± 0.07 (Rose et al., 2010)
NHI	[-]	N harvest index	$\frac{N_{grain}}{N_{shoot}}$	0.66 ± 0.11 (Van Duivenbooden, 1992)	0.73 ± 0.03 (Górny & Garczyński, 2008)	0.61 ± 0.10 (Van Duivenbooden, 1992)
$N_{\%, grain}$	[gN/kgDM]	Grain N concentration	$\gamma . \frac{N_{grain}}{C_{grain}}$	15.5 ± 3.0 (Van Duivenbooden, 1992)	21.4 ± 4.8 (Van Duivenbooden, 1992)	11.7 (Ye et al., 2014)
$N_{\%, root}$	[gN/kgDM]	Root N concentration	$\gamma . \frac{N_{root}}{C_{root}}$	12.7 (Latshaw & Miller, 1924)	6.1 (Hocking, 1994)	13.4 ± 0.1 (Ye et al., 2014)
PHI	[-]	P harvest index	$\frac{P_{grain}}{P_{shoot}}$	0.67 ± 0.13 (Van Duivenbooden, 1992)	0.67 ± 0.07 (Górny & Garczyński, 2008)	0.61 ± 0.13 (Van Duivenbooden, 1992)
$P_{\%, grain}$	[gP/kgDM]	Grain P concentration	$\gamma . \frac{P_{grain}}{C_{grain}}$	2.90 ± 0.80 (Van Duivenbooden, 1992)	3.70 ± 0.80 (Van Duivenbooden, 1992)	3.58 ± 0.15 (Ye et al., 2014)
$P_{\%, root}$	[gP/kgDM]	Root P concentration	$\gamma . \frac{P_{root}}{C_{root}}$	1.20 (Latshaw & Miller, 1924)	1.01 (Hocking, 1994)	1.31 ± 0.21 (Ye et al., 2014)

Table S2. Global crop area and production provided by global datasets and considered in our study.

		Maize	Wheat	Rice
Crop area [Mha]	Observed crop area (Ramankutty et al., 2008) = CROP	142	214	168
	Observed crop area considered in our study * = CROP_f (n=number of grid-cells)	96 (n=11565)	158 (n=9891)	93 (n=6405)
Production [Mt of DM]	CROP x Potential yield provided by Mueller et al. (2012)	892	858	823
	CROP_f x Potential yield provided by Mueller et al. (2012)	661	647	473

* the reduction from CROP to CROP_f is totally explained by the exclusion of grid-cells without a soil P estimate in Ringeval et al. (2017), which prevents the computation of S_P and R_P. In Ringeval et al. (2017), some grid-cells are not considered because of missing data about farming practices in (Bouwman et al., 2011) in which a bolean treatment of cropland land-use lead to exclude grid-cells with very small cropland fraction.

Table S3. For all crops, global values of supply (*S*), demand (*D*) and supply/demand ratio (*R*) for N and P when the two nutrients are considered as independent. For all variables (*S*, *D*, *R*), we computed a global average weighted by the crop area for each simulation out of the 1000 replicates (see Text S5). Average (*AVG*), standard-deviation (*STD*) and coefficient of variation (*CV*) of the 1000 global averages are given in the Table. *AVG* and *STD* are in kg(N or P)/ha/yr while *CV* is in %.

		N	P
Maize	S	AVG = 140.99 STD = 1.77 CV = 1	AVG = 106.98 STD = 4.39 CV = 4
	D	AVG = 195.08 STD = 1.03 CV = 1	AVG = 33.84 STD = 0.26 CV = 1
	R	AVG = 0.52 STD = 0.00 CV = 0	AVG = 0.61 STD = 0.01 CV = 1
Wheat	S	AVG = 137.31 STD = 2.79 CV = 2	AVG = 189.63 STD = 6.21 CV = 3
	D	AVG = 128.22 STD = 0.51 CV = 0	AVG = 24.18 STD = 0.10 CV = 0
	R	AVG = 0.60 STD = 0.00 CV = 0	AVG = 0.72 STD = 0.01 CV = 1
Rice	S	AVG = 151.16 STD = 1.52 CV = 1	AVG = 76.23 STD = 2.29 CV = 3
	D	AVG = 121.14 STD = 0.90 CV = 1	AVG = 33.52 STD = 0.27 CV = 1
	R	AVG = 0.77 STD = 0.00 CV = 0	AVG = 0.77 STD = 0.01 CV = 1